cosmetics

MDPI

Article

Nanostructured Lipid Carriers Enhance In Vitro Skin Delivery of Enzymatically Extracted *Bombyx mori* Silk Cocoon Bioactives: Development and Clinical Evaluation of an Anti-Aging Facial Serum

Sarocha Chareegun [1] and Wantida Chaiyana [1,2,3,*]

[1] Department of Pharmaceutical Science, Faculty of Pharmacy, Chiang Mai University, Chiang Mai 50200, Thailand; sarocha_chareegun@cmu.ac.th
[2] Center of Excellence in Pharmaceutical Nanotechnology, Faculty of Pharmacy, Chiang Mai University, Chiang Mai 50200, Thailand
[3] Multidisciplinary and Interdisciplinary School, Chiang Mai University, Chiang Mai 50200, Thailand
* Correspondence: wantida.chaiyana@cmu.ac.th; Tel.: +66-63944343

Abstract

Background/Objectives: This study investigated the potential of nanostructured lipid carriers (NLCs) to improve the in vitro skin delivery and retention of bioactive compounds derived from *Bombyx mori* silk cocoon. Furthermore, an NLC-based facial serum was developed and clinically evaluated for its efficacy and safety. **Methods**: Silk cocoons from Nang Lai (NL) and Lueang Saraburi (LS) were extracted using aqueous and enzymatic methods. Extracts were evaluated for protein, phenolic, and flavonoid contents, antioxidant activity, collagenase inhibition, and irritation potential. The most active extract was incorporated into NLCs and assessed for their physicochemical properties, entrapment efficiency, release, and Strat-M® membrane permeation and retention. The selected NLC was subsequently incorporated into a facial serum and clinically evaluated in 30 volunteers over 28 days for its effects on skin hydration and roughness using a Corneometer® and Visioscan®, respectively. **Results**: Enzymatic extraction markedly increased phenolic and flavonoid contents, resulting in stronger antioxidant and collagenase inhibitory activities than aqueous extraction. LS enzymatic extract (LS-EN) exhibited the most favorable overall bioactivities and was selected for NLC formulation, which showed a particle size of 149 ± 1 nm, low polydispersity index (0.263 ± 0.05), a zeta potential of −48 ± 1 mV, and an entrapment efficiency of 83%. Compared with the solution, the NLCs showed sustained release and approximately 3.7-fold higher membrane retention (5.45 ± 0.59% versus 1.47 ± 0.59%). The NLC-based facial serum demonstrated good skin tolerability and high user satisfaction, with skin moisture increasing by 7.05% and skin roughness significantly decreasing by 6.74–7.29% after 28 days of application ($p < 0.05$). **Conclusions**: Enzymatic extraction combined with NLC encapsulation enhanced the cosmeceutical potential of silk cocoon bioactive by enabling sustained release and localized retention, while the NLC-based facial serum demonstrated good skin tolerability and improved skin hydration and roughness, supporting its potential as a promising anti-aging cosmeceuticals.

Keywords: agricultural sustainability; value-added agricultural products; nanostructured lipid carriers; nanotechnology; drug delivery system; controlled release; Strat M® membrane

Check for updates

Academic Editor: Enzo Berardesca

Received: 29 July 2026
Revised: 28 August 2026
Accepted: 7 September 2026
Published: 10 September 2026

Copyright: © 2026 by the authors. Licensee MDPI, Basel, Switzerland. This article is an open access article distributed under the terms and conditions of the Creative Commons Attribution (CC BY) license.

1. Introduction

Silkworm (*Bombyx mori*) cocoons represent a sustainable and biologically rich source of natural macromolecules with growing interest in pharmaceutical and cosmeceutical applications [1,2]. Silk powder is widely recognized for its moisturizing and skin-brightening properties, making it a common ingredient in cosmetic products [3]. The cocoon matrix is primarily composed of fibroin and sericin proteins, along with minor quantities of bioactive phytochemicals derived from mulberry leaf metabolites [2,4]. Among these, sericin has attracted significant attention due to its hydrophilic nature and reported antioxidant, moisturizing, and anti-aging properties, including inhibition of extracellular matrix-degrading enzymes (e.g., hyaluronidase, elastase, and collagenase) [5,6]. However, the functional performance of silk-derived extracts is highly dependent on their molecular composition, which is strongly influenced by both biological variability of silkworm strains and extraction processing conditions [7,8]. Previous studies have demonstrated that extraction methodology plays a critical role in determining the yield and bioactivity of silk cocoon extracts [9–11]. In particular, enzymatic hydrolysis has been shown to improve the release of sericin-derived peptides and co-extracted phenolic and flavonoid compounds, resulting in enhanced antioxidant and anti-collagenase activities compared with conventional aqueous extraction [12,13]. In our previous investigation [14], enzymatic extraction of *B. mori* silk cocoons was found to significantly enhance the recovery of phenolic and flavonoid constituents, leading to improved antioxidants and collagenase inhibitory activities while maintaining excellent biocompatibility. Nevertheless, that study was limited to a single silkworm strain (Nang Lai), thereby precluding assessment of strain-dependent variability in extraction efficiency, bioactive composition, and cosmeceutical performance [14]. Accordingly, this study extended our prior investigation by evaluating the combined effects of silkworm strain and extraction green solvent on the compositional profile, bioactivity, and safety characteristics of *B. mori* silk cocoon extracts.

There are various strains of *B. mori* that have been developed through natural variation and selective breeding, exhibiting distinct differences in cocoon morphology, pigmentation, growth performance, and biochemical composition [15,16]. Among these, the Nang Lai (NL) strain is a native Thai silkworm known for producing smaller, deeply pigmented yellow cocoons, whereas the Lueang Saraburi (LS) strain is a hybrid line derived from Thai Nang Lai and Japanese J108 strains, characterized by larger cocoon size and lighter coloration [17,18]. These genetic and phenotypic differences are expected to influence cocoon protein content, sericin yield, and the associated profile of bioactive compounds, which in turn may affect extraction efficiency and biological functionality. Accordingly, NL and LS were selected in the present study to represent contrasting native and hybrid genetic backgrounds, enabling an evaluation of how silkworm strain variation impacts the composition, bioactivity, and cosmeceutical potential of silk cocoon-derived extracts.

Although silk cocoon-derived extracts have demonstrated considerable potential for cosmetic applications, their practical use in topical formulations is limited by their predominantly hydrophilic nature, which hinders partitioning into the lipid-rich stratum corneum and consequently restricts skin permeation and bioavailability at the target site [19]. From a formulation standpoint, these limitations necessitate the development of advanced delivery systems capable of enhancing cutaneous localization while preventing transdermal permeation [20–22]. Nanostructured lipid carriers (NLCs) have therefore emerged as a promising dermal delivery platform due to their biocompatibility, ability to sustain drug release, and enhanced retention within superficial skin layers [23–25]. Their lipid-based composition, consisting of both solid and liquid lipids, creates an imperfect crystalline structure that increases drug-loading capacity and facilitates controlled diffusion of incorporated bioactives [26,27]. This structural feature also enhances interaction with the stratum

corneum lipids, promoting close adhesion to the skin surface and improving localization within the upper skin layers [28,29]. Importantly, NLCs are particularly suitable for topical applications where localized skin activity is desired, as they favor retention within the skin rather than systemic permeation [30,31]. Additionally, beyond the development of an effective delivery system, translating silk cocoon-derived bioactives into a practical cosmeceutical product requires incorporation into a suitable topical formulation. Facial serums represent a convenient vehicle for delivering bioactive ingredients to the skin and are widely used in anti-aging applications. However, the clinical performance of such formulations should be evaluated.

Therefore, the present study aimed to investigate the influence of silkworm strain (NL and LS) and extraction green solvent (aqueous and enzymatic solution) on the chemical composition, biological activities, and safety profile of *B. mori* silk cocoon extracts, and to further develop and evaluate the NLC system for the topical delivery of the most bioactive extract, with particular emphasis on its release behavior, membrane retention, and skin-mimicking permeation characteristics using Strat M® membrane. Furthermore, an NLC-based facial serum was developed and clinically evaluated for its skin tolerability, effects on skin hydration and roughness, sensory attributes, and user satisfaction.

2. Materials and Methods

2.1. Silk Cocoon Materials

Yellow silk cocoons (*B. mori*) from two strains, Nang Lai Saraburi (NL) and Lueang Saraburi (LS), were obtained from the Queen Sirikit Sericulture Center, Chiang Mai, Thailand. The corresponding silkworm strains were identified and authenticated by the Queen Sirikit Department of Sericulture, Thailand, prior to collection.

2.2. Chemical Materials

Bicinchoninic acid (BCA) protein assay kit, cupric sulfate, Alcalase® enzyme from *Bacillus licheniformis*, and sodium hydroxide (NaOH) were purchased from Merck KGaA (Darmstadt, Germany). Sodium carbonate (Na_2CO_3), calcium chloride ($CaCl_2$), disodium hydrogen phosphate (Na_2HPO_4), and sodium chloride (NaCl) were purchased from Thermo Fisher Scientific (Waltham, MA, USA). Folin–Ciocalteu reagent, ammonium persulfate, aluminum chloride ($AlCl_3$), potassium acetate (CH_3COOK), potassium persulfate ($K_2S_2O_8$) ferric chloride ($FeCl_3$), ferrous sulfate ($FeSO_4$), sodium phosphate, sodium acetate, phosphotungstic acid, and sodium lauryl sulfate (SLS) were purchased from Loba Chemie (Mumbai, India). Sericin standard from *B. mori*, L-ascorbic acid (purity $\geq$ 99.0%), gallic acid, quercetin, 2,2-diphenyl-1-picrylhydrazyl (DPPH), 2,2′-azino-bis(3-ethylbenzothiazoline-6-sulfonic acid) (ABTS), 2,4,6-tripyridyl-S-triazine (TPTZ), collagenase from *Clostridium histolyticum*, N-[3-(2-furyl)acryloyl]-Leu-Gly-Pro-Ala (FALGPA), epigallocatechin gallate (EGCG), and bovine serum albumin (BSA) were purchased from Sigma-Aldrich (St. Louis, MO, USA). Glyceryl monostearate (GMS), Oryza sativa bran oil, polysorbate 80 (Tween® 80), sorbitan oleate (Span® 80) were purchased from NamSiang Co., Ltd. (Bangkok, Thailand). Acetic acid, methanol, ethanol, and hydrochloric acid (HCl) were analytical-grade and purchased from RCI Labscan Co., Ltd. (Bangkok, Thailand).

2.3. Extraction of Bioactive Compounds from Silk Cocoon

Two *B. mori* strains, NL and LS, were extracted using aqueous (AQ) and enzymatic-assisted (EN) methods, yielding LS-AQ, LS-EN, NL-AQ, and NL-EN extracts.

2.3.1. Aqueous Extraction of Bioactive Compounds from Silk Cocoon

Silk cocoons were extracted using an aqueous extraction method modified from Chareegun et al. (2025) [14]. Prior to extraction, silk cocoons were cut into small fragments, soaked in DI water, and subjected to microwave pretreatment using a microwave oven (MWP-MM20P(WH), Toshiba Co., Ltd., Tokyo, Japan) at 700 W for 3 min. After the soaking water was removed, the pretreated silk cocoons were extracted with DI water at a solid-to-liquid ratio of 1:25 w/v by heating at 100 °C for 2 h, following the conventional hot-water extraction [32]. The resulting extract was allowed to cool to room temperature and then filtered through muslin cloth to remove insoluble residues. The filtrate was subsequently freeze-dried using an industrial-scale vacuum freeze dryer (Kinetic Engineering Co., Ltd., Bangkok, Thailand) to obtain dried silk cocoon extract. The extraction yield was calculated using the following equation:

$$\text{Yield (\%)} = (\text{A}/\text{B}) \times 100, \quad (1)$$

where A is the weight of the dried extract obtained after freeze-drying and B is the initial weight of the silk cocoons used for extraction. All experiments were performed in triplicate.

2.3.2. Enzyme-Assisted Extraction of Bioactive Compounds from Silk Cocoon

Silk cocoons were extracted using an enzyme-assisted extraction method modified from Chareegun et al. (2025) [14]. Briefly, each silk cocoon was cut into small pieces and immersed in DI water. Prior to extraction, silk cocoons from both strains were subjected to microwave pretreatment using a microwave oven (MWP-MM20P(WH), Toshiba Co., Ltd., Tokyo, Japan) at 700 W for 3 min. After removal of the water, the pretreated cocoons were extracted at a ratio of 1:25 w/v using a 0.5% v/v Alcalase® solution pH 8.0 at 50 °C for 2 h. The extract was then cooled to room temperature and filtered through muslin cloth. The resulting filtrate was freeze-dried using an industrial-scale vacuum freeze dryer (Kinetic Engineering Co., Ltd., Bangkok, Thailand). The extraction yield was calculated using the following equation:

$$\text{Yield (\%)} = (\text{A}/\text{B}) \times 100, \quad (2)$$

where A is the weight of the dried silk cocoon extract and B is the initial weight of the silk cocoons used for extraction. All experiments were performed in triplicate.

2.4. Chemical Compositions Analysis

2.4.1. Determination of Total Protein Content

The protein content of each silk cocoon extract was determined by the Dumas combustion method using a nitrogen analyzer (Dumatherm N Pro, Gerhardt GmbH & Co. KG, Königswinter, Germany) [33–35] and by a bicinchoninic acid (BCA) protein assay [36]. The nitrogen content measured by the Dumas method was converted to protein content using the conventional nitrogen-to-protein conversion factor of 6.25 [35]. The BCA assay was performed according to the manufacturer's instructions, with slight modifications [36], and protein content was quantified using a bovine serum albumin (BSA) standard curve. All experiments were performed independently in triplicate.

2.4.2. Determination of Total Phenolic Content (TPC) and Total Flavonoid Content (TFC)

TPC and TFC of each silk cocoon extract were determined using the Folin–Ciocalteu and aluminum chloride colorimetric methods, respectively, with absorbance measured using a microplate spectrophotometer (SPECTROstar Nano, BMG Labtech, Ortenberg, Germany) [37,38]. Gallic acid and quercetin were used as standards for TPC and TFC, respectively, and the results were expressed as mg gallic acid equivalent (GAE)/g extract and

mg quercetin equivalent (QE)/g extract. All measurements were performed independently in triplicate.

2.5. Determination of Cosmeceutical-Related Biological Activities of Silk Cocoon Extracts

2.5.1. Antioxidant Activity

The antioxidant activities of silk cocoon extracts were evaluated using the 2,2-diphenyl-1-picrylhydrazyl (DPPH) [39], 2,2′-azino-bis(3-ethylbenzothiazoline-6-sulfonic acid) (ABTS) [40], and ferric reducing antioxidant power (FRAP) assay [41]. Radical scavenging activity against $DPPH^{\bullet}$ and $ABTS^{\bullet+}$ was calculated as follows:

$$\text{Radical scavenging activity (\%)} = [(A - B)/A] \times 100, \quad (3)$$

where A and B represent the absorbance of the control and sample, respectively. The IC_{50} values were determined from the concentration–response curves of radical scavenging activity. On the other hand, FRAP was quantified using an $FeSO_4$ standard curve and expressed as $FeSO_4$ equivalent capacity (EC_1). Ascorbic acid was used as positive control. All measurements were performed independently in triplicate.

2.5.2. Collagenase Inhibition

Collagenase inhibitory activity was determined using a modified substrate–enzyme method according to Thring et al. (2009) [42]. Absorbance was kinetically measured at 340 nm using a microplate spectrophotometer (SPECTROstar Nano, BMG Labtech, Ortenberg, Germany). Inhibitory activity was calculated as follows:

$$\text{Collagenase Inhibition (\%)} = [(A - B)/A] \times 100, \quad (4)$$

where A and B represent the reaction rates of the control and sample, respectively. Epigallocatechin gallate (EGCG) was used as the positive control, and IC_{50} values were determined from the concentration–response curves. All measurements were performed independently in triplicate.

2.6. Irritation Test by Hen's Egg Test on Chorioallantoic Membrane (HET-CAM) Assay

The irritation potential of silk cocoon extracts was evaluated using HET-CAM method according to Luepke (1985) [43]. Fertilized hen's eggs (7–9 days old) were treated with 1% *w*/*w* silk cocoon extract, and vascular responses were observed for 5 min under a stereoscope (NS80, Ningbo Yongxin Optics, Ningbo, China). Irritation scores (ISs) were calculated based on the onset times of hemorrhage, vessel lysis, and coagulation, and classified according to Freire et al. (2015) [44]. Sodium lauryl sulfate (SLS, 1% *w*/*v*) and normal saline solution (NSS) were used as the positive and negative controls, respectively. All experiments were performed independently in duplicate.

2.7. Development of Nanostructured Lipid Carriers (NLCs)

Blank NLCs were prepared using the emulsification–ultrasonication technique as described by Shirazi et al. (2021), with some modifications [45]. The influence of the solid lipid-to-liquid lipid ratio on NLC formulation was investigated by preparing three formulations containing a total lipid content of 5% *w*/*w*. Glyceryl monostearate (GMS) served as the solid lipid, while rice bran oil was used as the liquid lipid at ratios of 9:1, 8:2, and 7:3. A surfactant system consisting of Tween® 80 and Span® 80 at a weight ratio of 1:2 was employed, giving a total surfactant concentration of 1.5% *w*/*w*. This corresponded to 0.5% *w*/*w* Tween® 80 and 1.0% *w*/*w* Span® 80. The lipid phase, composed of GMS, rice bran oil, and Span® 80, was heated to 80 °C. Separately, the aqueous phase containing

Tween® 80 and DI water was heated to 85 °C. The aqueous phase was then gradually added to the lipid phase under continuous mixing, followed by ultrasonication using a probe sonicator (VCX 600, Vibra-Cell, Sonics & Materials, Newtown, CT, USA) operated at 60% amplitude for 5 min in pulsed mode (10 s on and 2 s off). The resulting NLCs were allowed to cool to room temperature and were stored in tightly closed containers at 4 °C until further characterization.

2.8. Characterization and Stability of Blank NLCs

2.8.1. Determination of Particle Size, Polydispersity Index (PDI), and Zeta Potential

Blank NLCs were characterized for particle size and PDI by dynamic light scattering (DLS), while zeta potential was determined by electrophoretic light scattering using a Zetasizer Nano ZS (Malvern Instruments Ltd., Malvern, UK). The samples were diluted with DI water at a ratio of 1:100 prior to analysis to ensure adequate dispersion of individual particles. DI water was used as the dispersion medium to minimize potential interference from ions during zeta potential measurement. All measurements were performed in triplicate.

2.8.2. Stability Test

The physical stability of blank NLCs were assessed using a centrifugation method [46]. Briefly, 1 mL of each formulation was transferred into a microcentrifuge tube and centrifuged at 5000 rpm for 15 min using a mini centrifuge (MINI-10K+, Hangzhou Miu Instruments Co., Ltd., Hangzhou, China). Following centrifugation, the formulations were visually inspected for signs of physical instability, including phase separation, creaming, sedimentation, or aggregation. Additionally, accelerated stability testing was performed using eight heating–cooling cycles. Each cycle consisted of storage at 45 °C for 24 h, followed by storage at 4 °C for an additional 24 h. After completion of the cycles, the formulations were evaluated for changes in physical appearance, and their particle size, PDI, and zeta potential were determined using a Zetasizer Nano ZS (Malvern Instruments Ltd., Malvern, UK). All experiments were conducted in triplicate.

2.9. Development of Nanostructured Lipid Carriers (NLCs) Containing Silk Cocoon Extracts

The silk cocoon extract exhibiting the most potent cosmetic-related activities and favorable safety profile was incorporated into the optimal NLC formulation, which was selected based on its desirable characteristics, including a small particle size, narrow PDI, appropriate zeta potential, and good stability following centrifugation and accelerated heating–cooling cycle testing. The silk cocoon extract was incorporated at a concentration of 0.1% *w*/*w*, as this concentration exceeded the IC_{50} values for $DPPH^{\bullet}$ radical scavenging and collagenase inhibition, thereby ensuring biologically active levels of the extract in the formulation. In brief, the extract was dissolved in the aqueous phase and heated to 85 °C, after which it was gradually added to the lipid phase maintained at 80 °C. The resulting mixture was immediately subjected to ultrasonication using a probe sonicator (VCX 600, Vibra-Cell, Sonics & Materials, Newtown, CT, USA) operated at 60% amplitude for 5 min in pulsed mode (10 s on and 2 s off). The resulting silk cocoon extract-loaded NLC was subsequently characterized for their particle size, PDI, zeta potential, and morphology. Additionally, the physical stability was evaluated by centrifugation and accelerated heating–cooling cycle tests as described in Section 2.8.2.

2.10. Morphology Determination

The morphology of the optimized silk cocoon extract-loaded NLCs and their corresponding blank NLCs was examined using transmission electron microscopy (TEM) (JEM-2100 Plus, JEOL Ltd., Tokyo, Japan). The samples were diluted with DI water at a ratio of 1:10 prior to analysis. A drop of the diluted NLC dispersion was placed onto a

300-mesh copper grid and allowed air-dry at room temperature. Subsequently, the sample was stained with 1% *w*/*v* phosphotungstic acid prepared in DI water. Then the excess stain was removed using a 0.22 µm membrane filter. The prepared grids were then observed under TEM operated at an accelerating voltage of 100 kV at 30,000× magnification.

2.11. Determination of Entrapment Efficiency and Loading Capacity of Silkworm Cocoon Extract-Loaded NLCs

Entrapment efficiency and loading capacity were determined according to Yeerong et al. (2024), with some modifications [47]. Briefly, 2 mL of silk cocoon extract-loaded NLC was placed into a centrifugal filter unit (Amicon® Ultra-15, MWCO 100 kDa, Merck KGaA, Darmstadt, Germany) and centrifuged at 5000× *g* for 15 min at 25 °C. The filtrate containing unentrapped free protein was collected and the total protein content was quantified using a BCA assay as described above. The percentage of entrapment efficiency was calculated using the following equation:

$$\text{Entrapment efficiency (\% } w/w) = 100 \times (1 - \text{B/A}), \quad (5)$$

where A represents the total protein content, and B represents the free protein in the filtrate. The percentage of loading capacity was calculated using the following equation:

$$\text{Loading capacity (\% } w/w) = 100 \times (\text{A} - \text{B})/\text{C}, \quad (6)$$

where C represents the total weight of the lipid phase used in the NLC formulation. All experiments were performed in triplicate.

2.12. Irritation Test of NLC and the Corresponding Formulation Containing Silkworm Cocoon Extract

The irritation potential of NLC and the corresponding formulation containing silkworm cocoon extract were assessed using the HET-CAM method, as described in Section 2.6 [43]. The SLS solution (1% *w*/*v*) was employed as the positive control, while NSS served as the negative control. All experiments were conducted independently in duplicate.

2.13. Release Study

The release study of silk cocoon extract-loaded NLCs was performed according to the method of Garg et al. (2021), with slight modifications [48]. Briefly, 1 mL of silk cocoon extract-loaded NLCs was loaded into a 2.5 × 2.5 cm dialysis bag (Spectra/Por® 1 dialysis tubing, MWCO 6–8 kDa, Fisher Chemicals, Loughborough, UK) and immersed in 20 mL of phosphate-buffered saline (PBS, pH 5.5). The system was maintained at 32 °C under continuous stirring at 250 rpm using a multi-position magnetic stirrer (AM4, EOS Scientific Co., Ltd., Bangkok, Thailand). Samples were collected at predetermined time intervals (0.5, 1, 2, 4, 6, 8, and 24 h). At each sampling point, an equal volume of fresh PBS pH 5.5 was immediately added to maintain sink conditions. The total protein content of the collected samples was analyzed using the BCA assay as described above. Total protein content was selected as the marker for monitoring LS-EN release because proteinaceous components, particularly silk sericin, are major bioactive constituents of the silk cocoon extract [1]. A silk cocoon extract solution was used as a control, and the amount of protein released from the NLCs was compared with that of the control. All experiments were performed in triplicate.

2.14. Permeation and Strat-M® Membrane Retention of Silk Cocoon Extract-Loaded NLCs

2.14.1. Permeation Determination

Membrane permeation of silk cocoon extract-loaded NLCs was evaluated in comparison with the silk cocoon extract solution using a Franz diffusion cell apparatus (Velp Scientific Inc., Milano, Italy), according to the method of Arce et al. (2020), with slight modifications [49]. Strat-M® membrane (Merck Millipore Ltd., County Cork, Ireland), a synthetic non-animal-based membrane available as 25 mm discs, was employed as a diffusion barrier to avoid interference in protein quantification [50]. Briefly, 12 mL of receptor medium (PBS, pH 7.4) was maintained at 37 °C and continuously stirred at 200 rpm. The membrane was mounted onto the diffusion cell 30 min prior to the experiment to allow equilibration. Subsequently, 1 mL of each formulation was placed in the donor chamber. At predetermined time intervals (0.5, 1, 2, 4, 6, 8, and 24 h), 1 mL of receptor medium was withdrawn and immediately replaced with an equal volume of fresh PBS to maintain sink conditions. The collected samples were analyzed using the BCA assay as described above. The permeation profiles of the formulations across the Strat-M® membrane were compared with those of the silk cocoon extract solution. All experiments were performed in triplicate.

2.14.2. Strat-M® Membrane Retention Determination

Following the 24 h permeation study, the Strat-M® membrane was collected to determine the amount of retained protein with slight modifications [50]. The membrane was gently rinsed three times with PBS pH 7.4 to remove any residual formulation from its surface and then cut into small pieces. Subsequently, 1 mL of PBS pH 7.4 was added to the membrane fragments, and the mixture was vortexed for 2 min, followed by sonication for 30 min using an ultrasonic bath (Elma Schmidbauer GmbH, Singen (Hohentwiel), Germany) to facilitate protein extraction from the membrane. The samples were then centrifuged at 10,000× *g* for 20 min, and the resulting supernatant was collected for protein quantification using the BCA assay. The amount of protein retained within the Strat-M® membrane after application of the silk cocoon extract-loaded NLCs was compared with that of the silk cocoon extract solution. All experiments were performed in triplicate.

2.15. Development of Facial Serum Containing Silk Cocoon Extract-Loaded NLCs

Facial serum formulation incorporating LS-EN-loaded NLCs was developed using the compositions presented in Table 1. In brief, NLC was incorporated at a concentration of 10% *w*/*w*, resulting in a final concentration of the LS-EN of 0.01% *w*/*w*. The NLCs were prepared using the emulsification–ultrasonication technique as described by Yeerong et al. (2025) with slight modifications [51]. The facial serum formulation was characterized in terms of visual appearance by organoleptic inspection, viscosity using a rheometer equipped with a plate-and-plate geometry (P25) (Brookfield Engineering Laboratories, Middleboro, MA, USA), and pH using a pH meter (inoLab pH Level 2; WTW, Weilheim, Germany). Additionally, the physical stability of the facial serum formulation was evaluated using a centrifugation method [46]. Briefly, 1 mL of the formulation was centrifuged at 5000 rpm for 15 min using a mini centrifuge (MINI-10K+, Hangzhou Miu Instruments Co., Ltd., Hangzhou, China), followed by visual examination for any signs of physical instability. Accelerated stability was further evaluated by subjecting the facial serum formulation to eight heating–cooling cycles. Following the stability testing, the physical properties of the formulation were assessed based on its visual appearance, pH, and viscosity.

Table 1. Ingredients of facial serum containing silk cocoon extract-loaded NLCs.

Ingredients	Concentration (% *w*/*w*)	Function
LS-EN NLC	10	Encapsulated bioactive
Carbopol® 940	0.4	Thickening agent
Spectrastat® BHL	3	Preservative
Triethanolamine	0.2	Neutralizer
Deionized water	q.s. 100	Solvent

Note: Carbopol® 940 = Carbomer; Spectrastat® BHL = Caprylhydroxamic acid (and) 1,2-hexanediol (and) butylene glycol; q.s. = quantum satis (quantity sufficient to the desired final amount).

2.16. Clinical Evaluation

2.16.1. Ethical Approval

A clinical study was conducted to evaluate the safety, efficacy, and satisfaction of a facial serum containing silk cocoon extract-loaded NLCs. The study was approved by the Ethics Committee of the Faculty of Pharmacy, Chiang Mai University, Thailand, under protocol No. 014/2569/E. Written informed consent was obtained from all participants before enrollment.

2.16.2. Human Volunteers

Thirty healthy volunteers, including 10 males (33.3%) and 20 females (66.7%), aged 20–60 years, were enrolled in the study based on predefined eligibility criteria. Eligible participants were healthy adults with no history of allergic reactions to cosmetics, topical medications, or silk cocoon-derived products. Participants were excluded if they had any dermatological conditions affecting the face or outer upper arm, tattoos at the designated test sites, or a known history of hypersensitivity to silk cocoon-derived ingredients.

2.16.3. Skin Irritation Test

The skin irritation potential of facial serum containing silk cocoon extract-loaded NLCs was evaluated according to the OECD Guideline for Acute Dermal Irritation/Corrosion (2015) and ISO 10993-10:2010 [52]. Briefly, 20 µL of each test formulation, along with the positive control (20% *w*/*v* sodium lauryl sulfate) and negative control (distilled water), was placed into an 8 mm Finn Chamber® (test area approximately 50 mm^2, (SmartPractice, Phoenix, AZ, USA)). The patches were applied to the outer aspect of the left upper arm for 4 h. During the exposure period, participants were instructed to avoid wetting the test area. If a patch became detached, participants were instructed to notify the investigators immediately so that the remaining exposure time could be completed. After 4 h, the patches were removed, and the test sites were gently cleaned with distilled water and dried with tissue paper. Skin reactions, including erythema and edema, were assessed immediately after patch removal and again at 24, 48, and 72 h. The Primary Irritation Index (PII) was calculated according to the OECD guideline using the Draize scoring system [53]. Based on the calculated PII values, skin irritation was classified as non-irritating, slightly irritating, moderately irritating, or severely irritating.

2.16.4. Clinical Efficacy Evaluation

Following confirmation of skin compatibility, the clinical efficacy of the facial serum formulations was evaluated. Baseline skin conditions were assessed before product application using non-invasive instrumental techniques. Skin hydration was measured using a Corneometer® CM 825 (Courage+Khazaka electronic GmbH, Cologne, Germany) and wrinkle parameters were evaluated using a Visioscan® VC20 (Courage+Khazaka electronic GmbH, Cologne, Germany). Participants were instructed to apply the formulation evenly

over the entire face twice daily, in the morning and evening after facial cleansing, for 28 consecutive days. Clinical evaluations were performed at baseline (Day 0) and after 7, 14, and 28 days of product application using the same instrumental methods.

2.16.5. Subject Satisfaction Assessment

At the completion of the clinical study, participants completed a self-assessment questionnaire regarding their satisfaction with the product. Product performance and overall user satisfaction were evaluated using a five-point Likert scale, where mean scores of 4.50–5.00, 3.50–4.49, 2.50–3.49, 1.50–2.49, and 1.00–1.49 indicated very high, high, moderate, low, and very low satisfaction, respectively [54].

2.17. Statistical Analysis

Data were expressed as mean ± standard deviation (S.D.) and sample differences were evaluated using one-way ANOVA followed by Tukey's post hoc test and a paired sample *t*-test conducted with IBM SPSS Statistics version 23.0 (SPSS Inc., Chicago, IL, USA). Statistical significance was set at $p < 0.05$.

3. Results and Discussion

3.1. Silk Cocoon Extracts

The morphological characteristics of the two silk cocoon strains are shown in Figure 1A. The NL cocoon originated from the native Thai silkworm strain, whereas the LS cocoon originated from a hybrid of the Thai Nang Lai and Japanese J108 strains [55]. The observations in the current study are consistent with previous reports describing the morphological characteristics of cocoons in *B. mori* [55–57]. Both strains exhibited the characteristic oval-shaped yellow cocoon morphology but differed in their size and coloration. The NL cocoon exhibited a deeper golden-yellow coloration, whereas the LS cocoon appeared lighter cream-yellow and was visually larger. The variation in silk cocoon coloration among strains is primarily driven by genetic differences affecting carotenoid uptake, transport, and deposition in sericin [18,58]. Previous study reported that the NL cocoon, derived from a native Thai strain, showed strong yellow coloration, whereas the J108 strain produces white cocoons [57]. The LS cocoon, a hybrid of NL and J108, exhibited a pale-yellow color, reflecting an intermediate phenotype [57]. Additionally, the hybrid LS strain has been reported to produce larger and heavier cocoons than native Thai yellow strains, as reflected by its greater cocoon and shell weights [56]. Soomherun et al. (2025) reported that the LS produced significantly heavier fresh cocoons, with an average weight of approximately 1.82 g, whereas the native Thai yellow strains, including Nangnoi Sisaket 1 and Tubtim-Siam, had average cocoon weights ranging from 0.89 to 0.97 g [56]. Furthermore, the larger cocoon size observed for the LS strain is likely attributable to the greater body size of the hybrid silkworm larva prior to pupation. As the cocoon is spun by the mature larva before metamorphosis, larger larvae generally produce larger cocoons, leading to increased cocoon and shell weights [59]. This explanation is supported by previous findings of Suraporn et al. (2015) showing that the LS exhibited a significantly greater fifth-instar larval weight (1.53 ± 0.05 g) than the native NL strain (1.18 ± 0.05 g), accompanied by a higher fresh cocoon weight (1.15 ± 0.00 g and 0.94 ± 0.07 g, respectively) [60]. These findings suggest that the greater larval body size of the hybrid strain contributes to the production of larger and heavier cocoons. Additionally, previous studies have reported that the native Thai NL strain produces female and male pupae with average sizes of approximately 10 mm × 18 mm and 8 mm × 14 mm, respectively, whereas the Japanese J108 strain produces larger pupae, measuring approximately 12 mm × 22 mm and 10 mm × 20 mm, respectively [61]. As the LS strain is a hybrid of Thai Nang Lai and

Japanese J108, its larger cocoon size may be attributed, at least in part, to the inheritance of favorable growth characteristics from the Japanese parental lineage, resulting in greater cocoon and shell weights than those of native Thai strains.

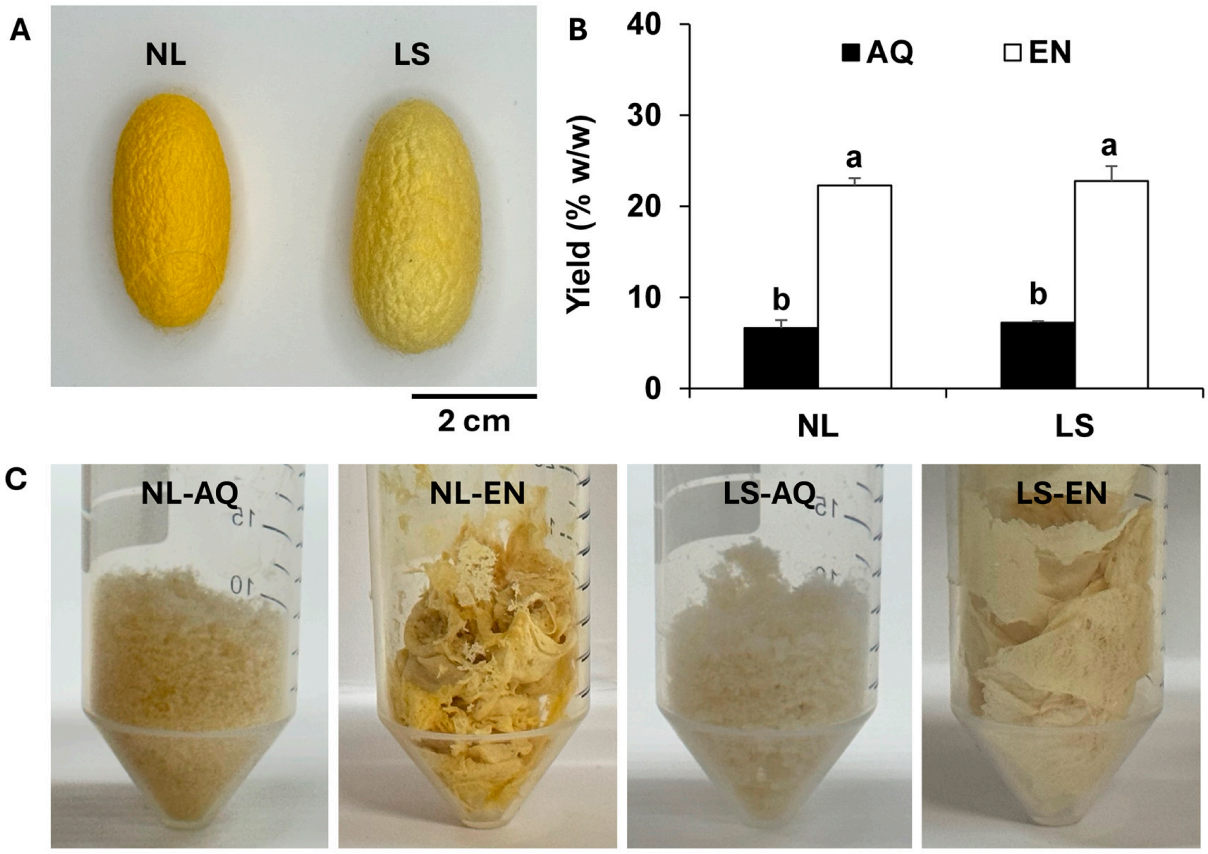


Figure 1. Representative appearance of two *B. mori* strains, Nang Lai Saraburi (NL) and Lueang Saraburi (LS) (scale bar = 2 cm) (**A**); extraction yields of silk cocoon extracts obtained using aqueous (AQ) and enzymatic (EN) extraction methods from the NL and LS strains (**B**); and representative photographs of the resulting silk cocoon extracts, including Nang Lai Saraburi aqueous extract (NL-AQ), Nang Lai Saraburi enzymatic extract (NL-EN), Lueang Saraburi aqueous extract (LS-AQ), and Lueang Saraburi enzymatic extract (LS-EN) (**C**). Different letters (a and b) indicate significant differences in extraction yield among the extracts ($p < 0.05$).

Both silk cocoons were successfully extracted using green solvents, including DI water and enzymatic solutions. The extraction yields of the silk cocoon extracts are shown in Figure 1B. Enzymatic extraction significantly increased the extraction yield compared with aqueous extraction in both cocoon strains ($p < 0.05$). The enzymatic-assisted extraction method produced yields of 22 ± 1% and 23 ± 2% w/w for NL and LS, respectively, whereas DI water yielded only 7% w/w. It was noted that no significant difference in extraction yield was observed between the NL and LS strains when the same extraction method was applied ($p > 0.05$), indicating that the extraction efficiency was primarily influenced by the extraction process rather than the cocoon strain. Silk cocoon consists mainly of fibroin and sericin, together with small amounts of non-sericin impurities and bioactive secondary metabolites such as flavonoids, alkaloids, coumarins, and phenolic acids, and has attracted increasing interest due to the biological properties of its major proteins [2]. Among these, sericin is now recognized as a valuable biomaterial and is recovered from silk through a degumming process that separates it from fibroin via hydrolytic or enzymatic cleavage of its peptide bonds using chemical, thermal, or biological methods [10]. Although sericin is insoluble in cold water, it readily undergoes hydrolysis in hot water, allowing its extraction

by conventional hot-water degumming [62]. However, hot-water extraction relies primarily on thermal hydrolysis, whereas enzymatic hydrolysis specifically cleaves peptide bonds, producing smaller peptides and free amino acids that enhance sericin solubilization and ultimately improve extraction efficiency [1,61].

On the other hand, the physical appearance of the extracted sericin varied with both the extraction method and cocoon strain, as shown in Figure 1C. The extraction method primarily influenced the morphology of the recovered sericin, whereas the cocoon strain mainly affected its color. The aqueous-extracted samples (NL-AQ and LS-AQ) appeared as loose, fine, granular, or fluffy precipitates with a relatively uniform texture. In contrast, the enzyme-assisted extracts (NL-EN and LS-EN) formed larger, cohesive, sponge-like aggregates with a denser and more compact structure. The enzyme-assisted extracts also exhibited a more intense yellow color, whereas the aqueous extracts appeared lighter. This may be attributed to the ability of enzymatic hydrolysis to more effectively disrupt the sericin matrix, facilitating the release of naturally occurring yellow pigments and other associated bioactive compounds, such as flavonoids (e.g., quercetin and kaempferol), that are present in silk cocoons [63]. Despite the similar morphologies observed within each extraction method, the NL extracts consistently displayed a deeper yellow coloration than the LS extracts, likely due to the naturally higher pigmentation of the NL silk cocoons.

3.2. Chemical Compositions of Silk Cocoon Extracts

The chemical compositions of silk cocoon extracts are presented in Table 2. Protein was identified as the major constituent of all silk cocoon extracts, with contents ranging from 40.4 $\pm$ 0.4% to 98.3 $\pm$ 0.5% w/w as determined by the BCA assay and 58.5 $\pm$ 0.0% to 95.0 $\pm$ 0.2% w/w by the N-analyzer. These findings are expected because the silkworm cocoon is primarily composed of two structural proteins, fibroin (75–83%) and sericin (17–25%), with sericin representing the principal water-soluble protein fraction recovered during the degumming process [64]. During degumming, either thermal or enzymatic treatment hydrolyzes peptide bonds within the sericin layer, allowing the protein to dissolve in water and separate from the insoluble fibroin fibers [65]. Among all samples, the aqueous extracts (NL-AQ and LS-AQ) contained significantly higher protein contents than the corresponding enzymatic extracts ($p < 0.05$), with LS-AQ showing the highest protein content by both analytical methods. The significantly lower protein content observed in the enzymatic extracts are likely attributable to proteolytic hydrolysis during extraction. Protease treatment hydrolyzes high-molecular-weight sericin into smaller peptides and free amino acids, altering the peptide length and amino acid environment. Although these hydrolysis products still contain nitrogen and are therefore quantified by the N-analyzer, extensive hydrolysis modifies the peptide bond structure and the reducing amino acid residues responsible for Cu^{2+} reduction in the bicinchoninic acid (BCA) assay, particularly cysteine, tyrosine, and tryptophan [66]. Consequently, the overall color-forming capacity of the hydrolysates is diminished, leading to a lower apparent protein content determined by the BCA assay compared with the nitrogen-based measurement. In contrast, the aqueous extracts showed comparable protein contents by both methods, suggesting that the extracted sericin remained largely intact and retained sufficient peptide structures to generate a BCA response comparable to that estimated from total nitrogen content.

Table 2. Total protein, phenolic, and flavonoid contents of silk cocoon extracts.

Samples	Protein Content (% *w*/*w*)		TPC (mg GAE per g Extract)	TFC (mg QE per g Extract)
	BCA Assay	N-Analyzer		
COM	78.3 ± 0.3 ^{c}	58.5 ± 0.0 ^{e,***}	20.9 ± 0.5 ^{d}	2.9 ± 0.4 ^{b}
NL-AQ	92.4 ± 0.6 ^{b}	89.2 ± 2.3 ^{b,NS}	23.6 ± 0.3 ^{c}	2.4 ± 0.6 ^{b}
NL-EN	40.4 ± 0.4 ^{e}	65.9 ± 0.1 ^{d,***}	31.2 ± 0.2 ^{b}	4.1 ± 1.0 ^{ab}
LS-AQ	98.3 ± 0.7 ^{a}	95.0 ± 2.1 ^{a,NS}	19.9 ± 0.3 ^{d}	3.1 ± 0.6 ^{b}
LS-EN	53.4 ± 0.3 ^{d}	79.8 ± 0.1 ^{c,***}	34.2 ± 0.5 ^{a}	5.1 ± 1.0 ^{a}

Note: Total protein content is expressed as % *w*/*w* determined by the bicinchoninic acid (BCA) assay and nitrogen (N) analyzer, total phenolic content (TPC) as mg gallic acid equivalent (GAE) per g extract, and total flavonoid content (TFC) as mg quercetin equivalent (QE) per g extract. COM = commercial sericin hydrolysate; NL-AQ = Nang Lai Saraburi aqueous extract; NL-EN = Nang Lai Saraburi enzymatic extract; LS-AQ = Lueang Saraburi aqueous extract; LS-EN = Lueang Saraburi enzymatic extract. Values are presented as mean ± standard deviation (SD) (n = 3). Different superscript letters (a–e) within the same column indicate significant differences among samples ($p < 0.05$) according to one-way ANOVA followed by Tukey's multiple comparison test. Asterisks indicate significant differences in total protein content determined by the BCA assay and the N-analyzer for the same sample, as assessed by a paired Student's t-test, *** = $p < 0.001$; NS = not significant ($p \geq 0.05$).

Interestingly, differences between the two silkworm strains were observed, although these were less pronounced than the effects of the extraction method. The LS strain consistently yielded significantly higher protein contents than the NL strain in both aqueous and enzymatic extracts, as determined by the BCA assay and the N-analyzer. These findings reveal that the extract obtained from the LS strain contained a higher protein content than that from the NL strain, suggesting greater sericin recovery during the extraction process. Consistent with this finding, previous studies have demonstrated that sericin recovery after degumming varies among *B. mori* strains, suggesting that genetic background influences the extractability of sericin [18]. These differences are typically attributed to variations in cocoon architecture and sericin localization, which influence the degree of sericin–fibroin interaction and ultimately influence the efficiency of sericin extraction [56,57]. However, the higher protein yield from the LS strain, predominantly composed of sericin, may be advantageous for biomaterial and cosmetic applications due to its well-known biocompatibility, moisture retention, and film-forming properties [67,68].

In addition to proteins, silk cocoon extracts may contain trace amounts of non-protein constituents, including flavonoids such as quercetin and kaempferol, as well as other low-molecular-weight compounds naturally associated with silkworm cocoons [69]. These phytochemicals are primarily derived from mulberry leaves consumed by silkworm larvae [70,71]. Quercetin has been reported to be absorbed from mulberry leaves, metabolized by the silkworm, and subsequently accumulated in the cocoon [71]. Therefore, the lower protein content observed in the enzymatic extracts may partly reflect the co-extraction of these non-protein constituents, thereby reducing the relative proportion of protein in the extracts. This interpretation is supported by the significantly higher total phenolic and flavonoid contents of the enzymatic extracts compared with their corresponding aqueous extracts, suggesting that enzymatic hydrolysis enhanced the release of cocoon-associated phytochemicals.

Protease treatment likely disrupted the sericin matrix and protein–phytochemical interactions, facilitating the liberation of low-molecular-weight phenolic compounds that may otherwise remain entrapped or bound within the protein network and increasing the recovery of naturally occurring antioxidant constituents associated with the cocoon [32]. Strain-dependent differences were also evident, with the LS strain exhibiting greater recovery of phenolic and flavonoid compounds than the NL strain following enzymatic

extraction. This observation suggests that the genetic background of *B. mori* may influence not only sericin recovery but also the abundance or extractability of cocoon-associated phytochemicals. Previous studies have reported that cocoon biochemical composition and sericin recovery vary among silkworm strains, reflecting differences in cocoon structure and metabolism [32]. Similarly, significant differences in the phenolic and flavonoid contents of the silk cocoon extracts have been reported among silkworm strains and species, indicating that genetic background influences the phytochemical composition of silk cocoons [72].

These findings indicate that enzymatic extraction enhances the recovery of phenolic and flavonoid compounds, which may contribute to greater antioxidant potential, while aqueous extraction preferentially preserves protein-rich sericin. Consequently, the choice of extraction method can be tailored according to the intended application and further biological evaluations, including antioxidants and skin-related bioactivity assays, are needed to confirm the functional significance of these compositional differences.

3.3. Cosmeceutical-Related Biological Activities of Silk Cocoon Extracts

The antioxidant capacity and collagenase inhibitory activity of the silk cocoon extracts are presented in Table 3. Different antioxidant assays, including FRAP, ABTS, and DPPH, were performed in the present study to evaluate the reducing power and radical scavenging capacity of the silk cocoon extracts through complementary electron-transfer and hydrogen-donation mechanisms, respectively. The FRAP assay measures the ability of antioxidants to reduce the Fe^{3+}–TPTZ complex to the blue-colored Fe^{2+}–TPTZ form, reflecting electron-donating (reducing) power under acidic conditions [73]. On the other hand, the ABTS and DPPH assays assess radical scavenging activity based on the ability of antioxidants to quench $ABTS^{\bullet+}$ and $DPPH^{\bullet}$ radicals via hydrogen atom or electron transfer, leading to a measurable decrease in absorbance [74]. These assays together provide a broad and reliable evaluation of the antioxidant potential of the extracts.

Table 3. Biological activities of silk cocoon extracts relevant to cosmeceutical applications.

Samples	EC_1 (μM $FeSO_4$ per g Extract)	IC_{50} (μg/mL)		
		DPPH• Inhibition	ABTS•+ Inhibition	Collagenase Inhibition
ASC	111 ± 1^{e}	1 ± 0^{a}	2 ± 0^{ab}	N/A
EGCG	N/A	N/A	N/A	27 ± 1^{a}
GAL	222 ± 1^{a}	0.2 ± 0.0^{a}	0.1 ± 0.0^{a}	248 ± 66^{a}
SER	N.D.	N.D.	54 ± 4^{c}	2616 ± 424^{d}
COM	16 ± 3^{g}	N.D.	53 ± 5^{c}	1586 ± 203^{c}
NL-AQ	126 ± 1^{d}	535 ± 50^{e}	118 ± 40^{d}	1286 ± 31^{bc}
NL-EN	174 ± 2^{c}	204 ± 2^{c}	42 ± 1^{bc}	246 ± 5^{a}
LS-AQ	59 ± 2^{f}	385 ± 20^{d}	150 ± 3^{d}	1047 ± 72^{b}
LS-EN	194 ± 1^{b}	98 ± 2^{b}	34 ± 1^{abc}	136 ± 3^{a}

Note: Equivalent concentration (EC_1) from the FRAP assay and half-maximal inhibitory concentration (IC_{50}) values are reported for ascorbic acid (ASC), gallic acid (GAL), epigallocatechin gallate (EGCG), standard sericin (SER); commercial sericin hydrolysate (COM), Nang Lai Saraburi aqueous extract (NL-AQ); Nang Lai Saraburi enzymatic extract (NL-EN), Lueang Saraburi aqueous extract (LS-AQ), and Lueang Saraburi enzymatic extract (LS-EN). Values are presented as mean ± standard deviation (SD) ($n = 3$). Different superscript letters (a–g) within the same column indicate significant differences among samples ($p < 0.05$) according to one-way ANOVA followed by Tukey's multiple comparison test. N/A = not applicable; N.D. = not detected.

Among the silk cocoon extracts, enzymatic extracts exhibited markedly greater antioxidant activity than the corresponding aqueous extracts, as demonstrated by higher ferric reducing antioxidant power (EC_1) and lower IC_{50} values for $DPPH^{\bullet}$ and $ABTS^{\bullet+}$

radical scavenging assays. In particular, the LS-EN extract showed the strongest antioxidant performance among all sericin extracts, followed by NL-EN, whereas both aqueous extracts displayed substantially weaker activities. Interestingly, LS-EN exhibited the highest ferric reducing antioxidant power among all silk cocoon extracts, with a value exceeding that of ascorbic acid ($p < 0.05$). This indicates a remarkably strong electron-donating and reducing capacity of the LS-EN extract within the FRAP assay system. The markedly higher FRAP activity observed in LS-EN is therefore more closely associated with phenolic constituents, as gallic acid (used as a representative standard for phenolic compounds) exhibited strong reducing capacity, whereas sericin (used as a representative standard for silk proteins) showed negligible contribution to the FRAP response. Accordingly, the enhanced reducing power of LS-EN is likely driven predominantly by phenolic compounds co-extracted alongside silk proteins rather than by sericin itself.

Similar trends were also observed in the radical scavenging assays, where gallic acid demonstrated markedly stronger activity than sericin, confirming phenolic compounds as the primary contributors to antioxidant effects. Consistently, LS-EN exhibited the lowest IC_{50} values among all silk cocoon extracts, indicating the strongest radical scavenging capacity. Although its activity did not surpass that of the positive control or standard antioxidant compounds, it was clearly more potent than sericin and the commercial sericin hydrolysate. This suggests that the superior antioxidant performance of LS-EN is not solely due to sericin content but is likely enhanced by co-extracted phenolic and flavonoid constituents, whereas the commercial sample may contain a more purified sericin fraction with limited associated phytochemicals. The IC_{50} values of LS-EN in DPPH and ABTS assays, corresponding to approximately 0.0098% and 0.0033% w/v, respectively, indicate strong radical scavenging activity at very low concentrations. These values fall within the effective range typically observed for antioxidant ingredients used in cosmetic formulations. Although not comparable to pure standard antioxidants, the activity is considerably higher than that of sericin alone, suggesting that LS-EN is a promising natural antioxidant candidate for further formulation development.

Additionally, collagenase inhibition was further evaluated as an additional anti-aging mechanism alongside antioxidant activity. Collagenase, particularly matrix metalloproteinase-1 (MMP-1), is a key enzyme responsible for the initial cleavage of type I collagen in the extracellular matrix, and its overexpression is strongly associated with skin aging and wrinkle formation due to progressive dermal collagen degradation [75,76]. Therefore, inhibition of collagenase activity is considered a critical strategy for preserving skin structural integrity and delaying visible aging [77]. A similar trend to that observed in the antioxidant assays was also evident in collagenase inhibition, with enzymatic extracts showing consistently higher activity than aqueous extracts. As summarized in Table 3, LS-EN exhibited the strongest collagenase inhibitory activity, followed by NL-EN, whereas both aqueous extracts and the commercial sericin hydrolysate showed comparatively weaker effects. This indicates that the observed bioactivity is not solely attributable to sericin but is significantly influenced by additional bioactive constituents released or co-extracted during enzymatic hydrolysis. Although the enzymatic extracts did not reach the potency of EGCG, they demonstrated markedly higher activity than gallic acid and standard sericin, highlighting their improved functional performance as natural collagenase inhibitors. Notably, LS-derived extracts consistently outperformed NL-derived extracts under both extraction conditions, suggesting that genetic background influences the availability of collagenase-inhibiting constituents. Therefore, enzymatic extraction, particularly from the LS strain, yields silk cocoon extracts with superior anti-collagenase potential, supporting their promise for anti-aging cosmeceutical applications. The low IC_{50} value of LS-EN (136 μg/mL, equivalent to approximately 0.0136% w/v) suggests that effective

collagenase inhibition can be achieved at concentrations substantially lower than those typically used for cosmetic active ingredients, supporting its potential for incorporation into anti-aging skincare formulations.

The superior antioxidants and anti-collagenase activities of the enzymatic extracts are consistent with their chemical composition. As shown in Table 2, both NL-EN and LS-EN contained significantly higher total phenolic and flavonoid contents than their corresponding aqueous extracts, whereas the aqueous extracts retained substantially higher protein contents. Phenolic compounds and flavonoids are well recognized as major contributors to reducing power and free radical scavenging activity owing to their hydrogen- and electron-donating abilities [78,79]. Consequently, the enhanced antioxidant capacity of the enzymatic extracts is likely attributable to the increased recovery of these phytochemicals during proteolytic hydrolysis. In contrast, aqueous extraction preferentially recovered protein-rich sericin but extracted fewer antioxidant phytochemicals, resulting in comparatively weaker antioxidant activity. The findings were consistent with our previous study, which suggested that enzymatic extraction enhanced the recovery of bioactive compounds from silkworm cocoons, thereby improving cosmeceutical properties including antioxidant, anti-aging, and moisturizing activities [14]. However, the present study extends previous work by comparing two genetically distinct strains (NL and LS), revealing clear strain-dependent differences in bioactive composition and activity. In particular, the hybrid LS strain showed higher phenolic and flavonoid contents, leading to superior antioxidant and collagenase inhibitory activities, especially under enzymatic extraction. This highlights the important role of genetic background in influencing cocoon phytochemical extractability, beyond extraction conditions alone. Under both extraction methods, the LS strain generally exhibited stronger antioxidant and collagenase inhibitory activities than the NL strain, particularly following enzymatic extraction. These findings correspond well with the higher total phenolic and flavonoid contents of LS-EN compared with NL-EN, suggesting that the hybrid LS strain possesses a greater abundance or extractability of antioxidant phytochemicals. Since sericin itself has only moderate antioxidant activity, as reflected by the relatively weak activity of the standard sericin and commercial sericin hydrolysate, the enhanced bioactivities observed in the enzymatic extracts are likely attributable to the combined effects of sericin-derived peptides together with cocoon-associated phenolic and flavonoid compounds. Therefore, these results demonstrate that the extraction method exerts a greater influence than silkworm strain on biological activity, although the LS strain consistently provided extracts with superior antioxidant potential. Among all samples, LS-EN exhibited the most favorable overall bioactivity and is recommended for further developed into cosmeceutical formulations.

3.4. Irritation Potentials of Silk Cocoon Extracts

The irritation potential of the silk cocoon extracts was evaluated using the HET-CAM test, a well-established alternative to in vivo animal testing for assessing the safety of cosmetic and pharmaceutical ingredients [80,81]. The assay employs the highly vascularized CAM of developing chicken embryos, which share structural and physiological characteristics with the human cornea, enabling sensitive detection of irritation responses, including hemorrhage, vessel lysis, and coagulation [82]. Due to its high sensitivity, rapidity, reproducibility, and good correlation with conventional in vivo irritation tests, the HET-CAM assay has been widely adopted for the safety evaluation of cosmetic ingredients and formulations, particularly skincare products [80,81]. Furthermore, because avian embryos are not classified as laboratory animals during the first two-thirds of embryonic development under Directive 2010/63/EU, the HET-CAM assay provides an ethical approach for irritation assessment without requiring animal ethics committee approval [83].

Representative images of the CAM following exposure to the test substances are presented in Figure 2. As expected, the positive control (1% *w*/*v* sodium lauryl sulfate) rapidly induced all the characteristic irritation responses, including hemorrhage, vessel lysis, and coagulation within 5 min of exposure, with the severity increasing after 60 min. Consistent with these observations, the positive control was classified as a severe irritant with the irritation score of 15.1 ± 0.3 as shown in Table 4. In contrast, the negative control (0.9% *w*/*v* sodium chloride) produced no observable vascular damage throughout the experiment (Figure 2) and was classified as non-irritating with an irritation score of 0.0 ± 0.0 (Table 4). All silk cocoon extracts, together with the commercial sericin hydrolysate and standard sericin, exhibited no visible signs of hemorrhage, coagulation, or vascular lysis, even after 60 min of continuous exposure. The blood vessels remained intact and well organized, with no apparent disruption of the CAM. These observations indicate that neither the extraction method nor the silkworm strain introduced detectable irritation to the CAM. The findings are consistent with previous reports demonstrating the excellent biocompatibility of sericin-based materials and silk protein extracts intended for cosmetic and biomedical applications [1,84,85]. Combined with their potent antioxidant and anti-collagenase activities, especially for LS-EN, the absence of observable irritation further supports the potential of enzymatically extracted silk cocoon proteins as multifunctional active ingredients for anti-aging cosmeceutical formulations.

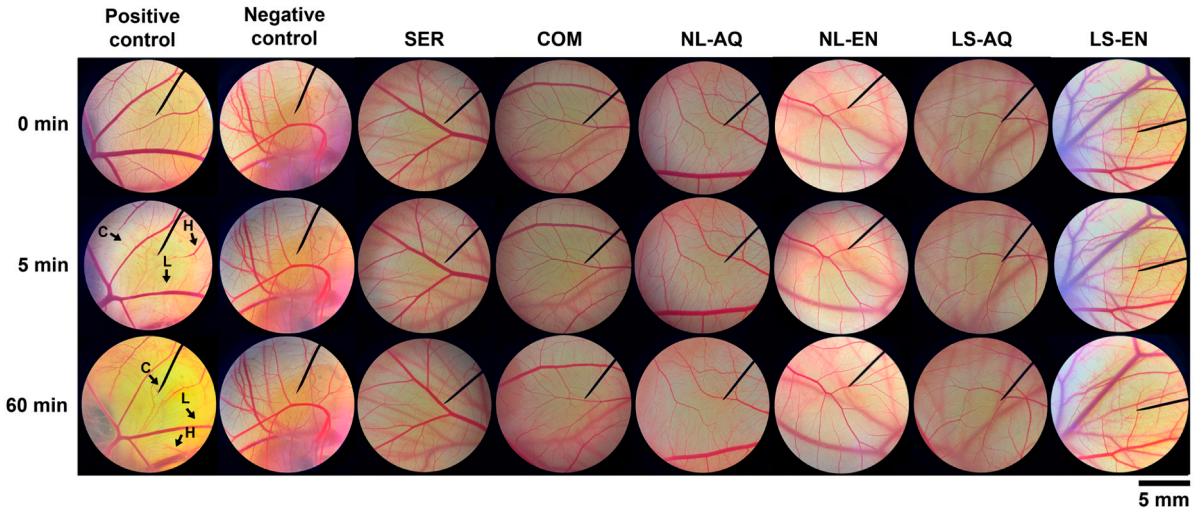


Figure 2. Representative images of the hen's egg chorioallantoic membrane (CAM) at 0, 5, and 60 min following exposure to the positive control (1% *w*/*v* sodium lauryl sulfate), negative control (0.9% *w*/*v* sodium chloride), standard sericin (SER), commercial sericin hydrolysate (COM), Nang Lai aqueous extract (NL-AQ), Nang Lai enzymatic extract (NL-EN), Lueang Saraburi aqueous extract (LS-AQ), and Lueang Saraburi enzymatic extract (LS-EN). The letters H, L, and C denote hemorrhage, lysis, and coagulation, respectively. Images were observed and captured under a stereomicroscope with a 10× objective magnification. Scale bar = 5 mm.

Notably, LS-EN were classified as non-irritating in the HET-CAM assay at a test concentration of 1% *w*/*v* (accounted for 10,000 µg/mL). This concentration is approximately 102×, 299×, and 74× higher than the IC_{50} values for DPPH, ABTS, and collagenase inhibition, respectively. These findings demonstrate a substantial safety margin between the biologically active concentrations and the irritation threshold, indicating a favorable safety profile. Accordingly, LS-EN at the concentration of 1% *w*/*v* would be recommended for further development as a promising cosmeceutical active ingredient.

Table 4. Irritation score and irritation potential of silk cocoon extracts.

Samples	Irritation Score	Irritation Potential
Positive control	15.1 ± 0.3 [a]	Severe irritation
Negative control	0.0 ± 0.0 [b]	No irritation
SER	0.0 ± 0.0 [b]	No irritation
COM	0.0 ± 0.0 [b]	No irritation
NL-AQ	0.0 ± 0.0 [b]	No irritation
NL-EN	0.0 ± 0.0 [b]	No irritation
LS-AQ	0.0 ± 0.0 [b]	No irritation
LS-EN	0.0 ± 0.0 [b]	No irritation

Note: Positive control = 1% *w*/*v* sodium lauryl sulfate, negative control = 0.9% *w*/*v* sodium chloride, SER = standard sericin, COM = commercial sericin hydrolysate, NL-AQ = Nang Lai aqueous extract, NL-EN = Nang Lai enzymatic extract, LS-AQ = Lueang Saraburi aqueous extract, and LS-EN = Lueang Saraburi enzymatic extract. Values are presented as mean ± standard deviation (SD) (n = 3). Different superscript letters (a and b) within the same column indicate significant differences among samples ($p < 0.05$) according to one-way ANOVA followed by Tukey's multiple comparison test.

3.5. Blank NLCs

NLC formulations were successfully developed using GMS as the solid lipid and rice bran oil as the liquid lipid. The effect of the solid lipid-to-liquid lipid ratio on the physicochemical characteristics and physical stability of NLC formulations was investigated, and the results are presented in Figure 3. Visual inspection revealed that all formulations formed homogeneous milky-white dispersions without visible phase separation immediately after preparation. Following centrifugation, the NLCs retained their uniform appearance with no evidence of creaming, sedimentation, or oil separation, suggesting good physical stability regardless of the lipid ratio. The particle size of freshly prepared NLCs ranged from approximately 138 ± 1 to 145 ± 1 nm (Figure 3B). Increasing the proportion of rice bran oil from a GMS-to-oil ratio of 9:1 to 7:3 significantly reduced particle size ($p < 0.05$), with the 7:3 formulation exhibiting the smallest nanoparticles. The reduction in particle size may be attributed to the increased liquid lipid content, which decreases the viscosity of the molten lipid phase during homogenization and ultrasonication [86]. As NLCs are nanoemulsion-based systems in which the lipid phase is partially or completely solidified, a lower molten lipid viscosity enables more efficient droplet disruption during emulsification, producing smaller nanoparticles upon solidification [87]. Moreover, increasing the liquid lipid fraction generates a less-ordered lipid matrix, which is characteristic of NLCs and contributes to improved encapsulation of lipophilic compounds while maintaining nanoparticle stability [88,89]. Following the accelerated stability test under heating–cooling conditions, the particle sizes of the 9:1 and 8:2 formulations increased significantly ($p < 0.001$), whereas the 7:3 formulation showed no significant change. The slight increase in particle size for the two formulations containing higher GMS levels may indicate minor particle association or aggregation. In contrast, the 7:3 formulation maintained its original particle size, suggesting superior stability.

On the other hand, the PDI values of all NLC formulations were relatively low, ranging from approximately 0.23 ± 0.02 to 0.27 ± 0.01 (Figure 3C), indicating narrow particle size distributions and successful nanoparticle production. No statistically significant differences in PDI were observed among the three formulations, either before or after centrifugation, demonstrating that modification of the lipid ratio did not adversely affect particle uniformity. In addition, all NLC formulations exhibited highly negative zeta potentials, ranging from approximately −40 to −46 mV (Figure 3D), which are generally considered sufficient to provide strong electrostatic repulsion and maintain colloidal stability. The zeta potential is widely recognized as a quantitative indicator of charge-induced colloidal stability, as it

reflects the magnitude of electrostatic repulsion between nanoparticles [90]. In general, zeta potential values between ±30 and ±40 mV indicate moderate electrostatic stability, whereas values exceeding ±40 mV are considered to provide sufficient electrostatic repulsion to maintain stable nanoparticle dispersions [90]. Therefore, the highly negative zeta potential values observed in all formulations suggest excellent colloidal stability and a low tendency for particle aggregation. Increasing the proportion of rice bran oil resulted in a significantly more negative zeta potential, with the 7:3 formulation showing the highest absolute value of −46 ± 2 mV. This enhancement may be attributed to the greater contribution of ionizable free fatty acids and other polar lipid constituents present in rice bran oil at the particle surface, thereby increasing the negative surface charge [91]. Importantly, the accelerated stability test under heating–cooling conditions did not significantly alter the zeta potential of any NLC formulation, indicating that the surface characteristics of the nanoparticles remained stable throughout the stress conditions.

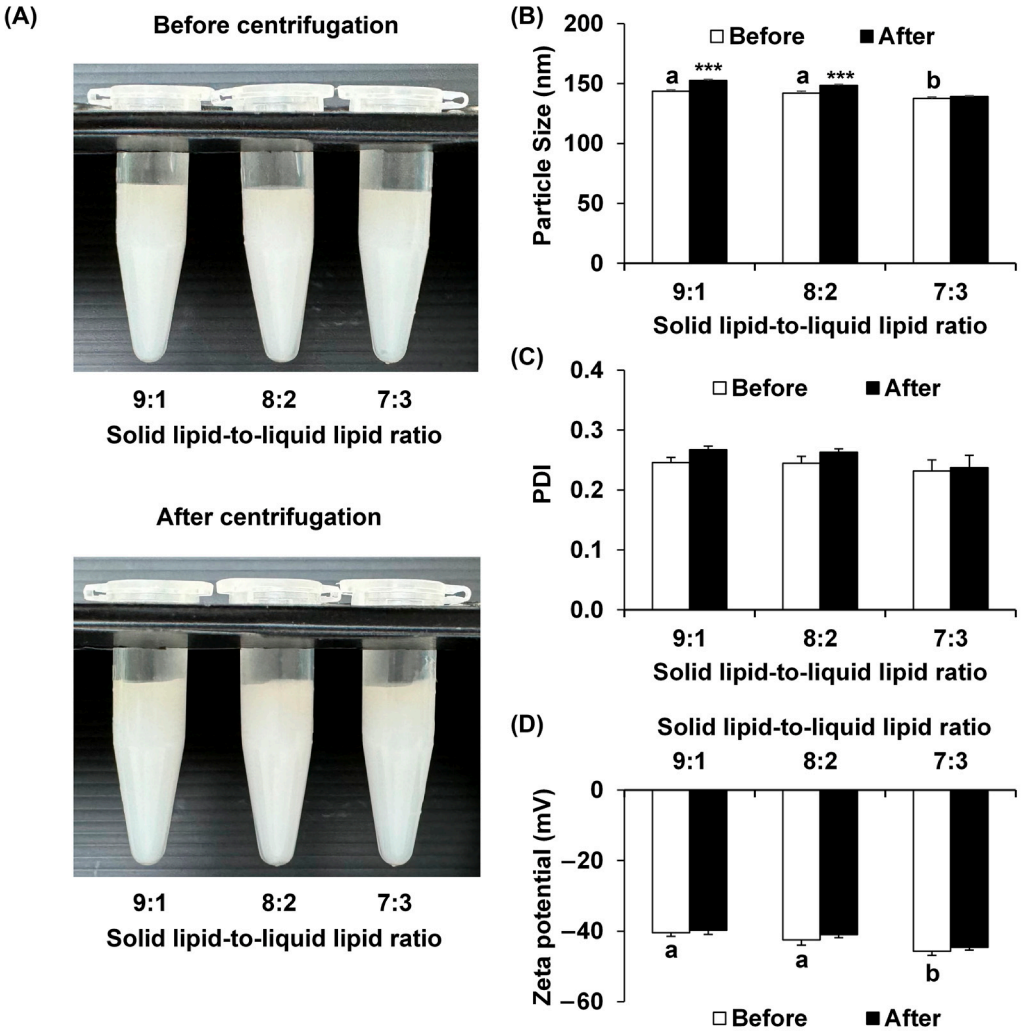


Figure 3. Effect of the solid lipid-to-liquid lipid ratio on the physicochemical properties and physical stability of nanostructured lipid carriers (NLCs). Representative photographs of NLCs prepared using glyceryl monostearate (GMS) and rice bran oil at solid lipid-to-liquid lipid ratios of 9:1, 8:2, and 7:3 before and after centrifugation (**A**), and the corresponding particle size (**B**), polydispersity index (PDI) (**C**), and zeta potential (**D**) of freshly prepared NLCs (white bars) and NLCs after centrifugation (black bars). Data are presented as mean ± SD (n = 3). Different lowercase letters (a and b) indicate significant differences among formulations before centrifugation ($p < 0.05$), while asterisks indicate significant differences between freshly prepared NLCs and NLCs after eight cycles of heating-cooling condition within the same formulation (***, $p < 0.001$).

Based on its significantly smaller particle size, acceptable PDI, and the most pronounced negative zeta potential, the formulation containing a 7:3 ratio of GMS to rice bran oil was selected for subsequent active ingredient incorporation. Furthermore, the higher proportion of liquid lipid is expected to create a more imperfect lipid matrix, thereby providing greater accommodation space for active compounds and enhancing encapsulation efficiency [92].

3.6. NLCs Containing Silk Cocoon Extracts

Silk cocoon extract-loaded NLC was successfully developed with an LS-EN concentration of 1% *w*/*v* as this concentration exhibited no irritation in the HET-CAM assay and provided a wide safety margin relative to the concentrations required for antioxidant and anti-collagenase activities, supporting its suitability as a cosmeceutical active ingredient. As shown in Figure 4A,B, both blank NLCs and silk cocoon extract-loaded NLCs exhibited a homogeneous milky-white appearance with no visible phase separation or sedimentation before and after centrifugation. The comparable appearance and stability of both formulations indicate that incorporation of the silk cocoon extract did not compromise the physical stability of the NLC system, suggesting successful encapsulation of the extract. The TEM micrographs (Figure 4C,D) showed that both blank and silk cocoon extract-loaded NLCs consisted of predominantly spherical particles with smooth surfaces and no apparent aggregation. The incorporation of LS-EN did not produce noticeable changes in particle morphology, indicating that nanoparticle formation was not adversely affected by extract loading. However, TEM images revealed that the silk cocoon extract-loaded NLCs exhibited a larger particle size than the blank NLCs, which was consistent with the DLS results showing average particle sizes of 138 $\pm$ 1 nm and 149 $\pm$ 1 nm, respectively (Figure 4E). The increase in particle size indicates successful encapsulation of the LS-EN within the lipid matrix rather than surface adsorption, a finding that is further supported by the high entrapment efficiency (83.0 $\pm$ 0.1%). In contrast, the loading capacity was relatively low (0.73 $\pm$ 0.00%). This can be attributed not only to the high lipid-to-extract ratio used in the formulation but also to the hydrophilic nature of LS-EN. As a water-soluble extract, LS-EN has a greater affinity for the aqueous phase than for the lipid matrix during nanoparticle preparation, thereby limiting the amount that can be incorporated into the lipid core. This observation is consistent with the fundamental characteristics of NLCs, which are generally more suitable for encapsulating lipophilic compounds because of their high compatibility with the lipid matrix [93]. Consequently, hydrophilic compounds typically exhibit lower loading capacities due to their limited partitioning into the lipid phase [93]. Nevertheless, the optimized formulation was able to retain a high proportion of the incorporated LS-EN, resulting in a high entrapment efficiency despite the relatively low loading capacity. These findings demonstrate that, although NLCs are not ideal carriers for maximizing the loading of hydrophilic compounds, they can still efficiently encapsulate and retain such bioactives when the formulation is appropriately developed, making them suitable for topical delivery applications.

On the other hand, the incorporation of LS-EN had no significant effect on the PDI or zeta potential of the NLCs. The PDI values remained low (0.214 $\pm$ 0.019 for blank NLCs and 0.260 $\pm$ 0.005 for silk cocoon extract-loaded NLCs), indicating a narrow particle size distribution and a homogeneous nanoparticle population. These findings are consistent with the TEM observations, which revealed uniformly shaped nanoparticles without noticeable aggregation, suggesting that the incorporation of silk cocoon extract did not compromise the homogeneity of the formulation. The zeta potential results (Figure 4G) further confirmed the colloidal stability of both formulations. Blank and silk cocoon extract-loaded NLCs exhibited comparable negative surface charges of -46 ± 2 mV and -48 ± 1 mV, respec-

tively. The absence of a significant difference in zeta potential indicates that incorporation of the extract did not alter the surface characteristics of the nanoparticles. Moreover, the high absolute zeta potential values (>30 mV) provided sufficient electrostatic repulsion to prevent particle aggregation, thereby contributing to the physical stability of the NLCs [94]. The physicochemical stability of the NLCs was further demonstrated by the accelerated heating–cooling stability test, during which no visible changes. These results indicate that both blank and silk cocoon extract-loaded NLCs maintained their physical stability under accelerated stress conditions, confirming that the incorporation of silk cocoon extract did not adversely affect the stability of the NLC system.

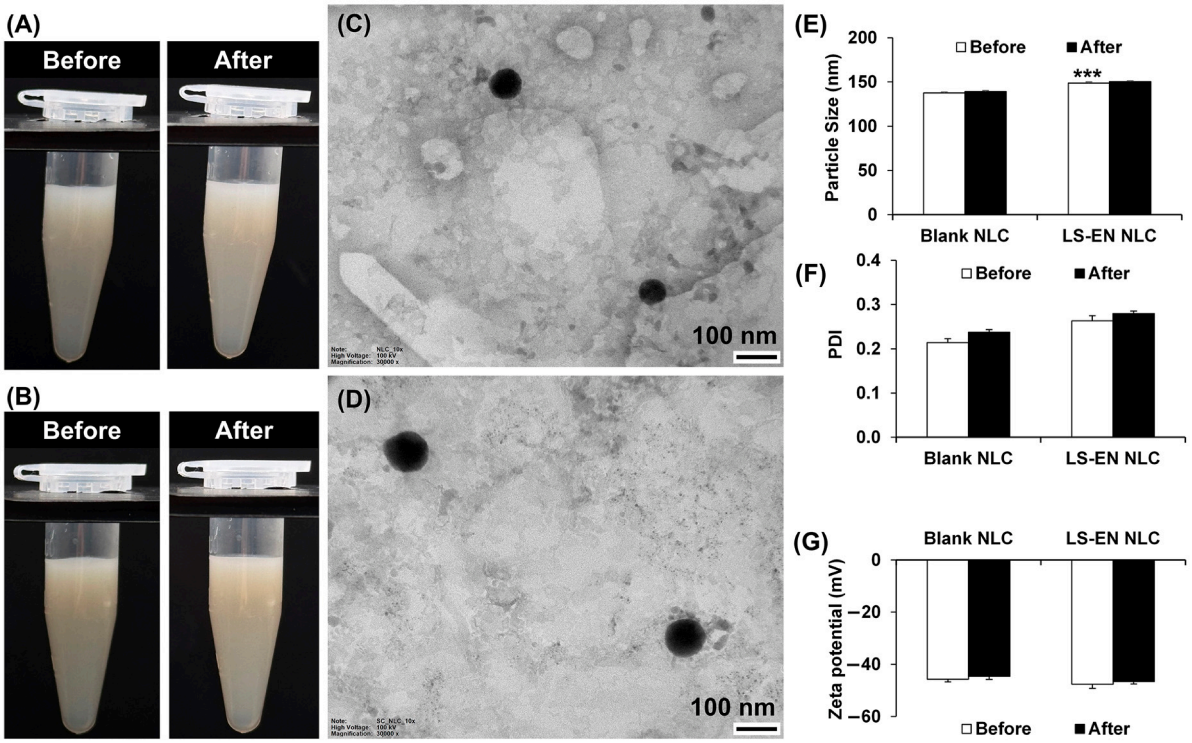


Figure 4. Visual appearance of blank nanostructured lipid carriers (NLCs) formulated with glyceryl monostearate (GMS) and rice bran oil at a 7:3 ratio (**A**) and the corresponding silk cocoon extract-loaded NLCs (**B**), before and after centrifugation. Transmission electron microscopy (TEM) micrographs (30,000× magnification) of the blank NLCs (**C**) and silk cocoon extract-loaded NLCs (**D**), along with the corresponding particle size (**E**), polydispersity index (PDI) (**F**), and zeta potential (**G**) of freshly prepared NLCs (white bars) and NLCs after centrifugation (black bars). Data are presented as the mean ± SD (n = 3). Asterisks indicate significant differences between freshly prepared NLCs and NLCs subjected to eight heating–cooling cycles within the same formulation (***, $p < 0.001$).

3.7. Irritation Potentials of NLCs Containing Silk Cocoon Extracts

The irritation potential of the blank NLC and LS-EN-loaded NLC was evaluated using the HET-CAM assay, and representative images are shown in Figure 5, while the corresponding irritation scores are presented in Table 5. The positive control (1% w/v sodium lauryl sulfate) induced severe irritation, characterized by rapid hemorrhage, vascular lysis, and coagulation of the CAM within the observation period, resulting in a high irritation score of 15.3 ± 0.3 ($p < 0.05$). In contrast, the negative control (0.9% w/v sodium chloride) produced no observable vascular damage and yielded an irritation score of 0.0 ± 0.0, confirming the validity of the assay. Similarly, both the blank NLC and LS-EN-loaded NLC exhibited no signs of hemorrhage, vascular lysis, or coagulation throughout the 60 min observation period (Figure 5). Consequently, both formulations received an irritation score of 0.0 ± 0.0. These findings indicate that neither the lipid carrier nor the

incorporation of 1% *w*/*w* LS-EN elicited irritation to the CAM. The absence of irritation following incorporation of LS-EN suggested that encapsulation within the NLC system did not adversely affect the biocompatibility of the formulation. Therefore, the silk cocoon extract-loaded NLC represents a promising nanocarrier for the topical delivery of LS-EN in cosmeceutical applications.

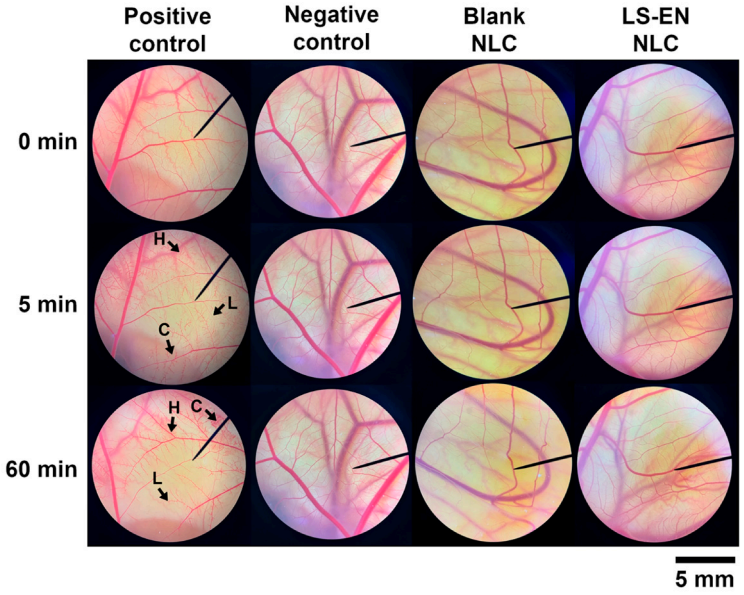


Figure 5. Representative images of the hen's egg chorioallantoic membrane (CAM) at 0, 5, and 60 min following exposure to the positive control (1% *w*/*v* sodium lauryl sulfate), negative control (0.9% *w*/*v* sodium chloride), blank nanostructured lipid carrier (Blank NLC), and nanostructured lipid carrier containing 1% *w*/*w* of Lueang Saraburi enzymatic extract (LS-EN NLC). The letters H, L, and C denote hemorrhage, lysis, and coagulation, respectively. Images were observed and captured under a stereomicroscope with a 10× objective magnification. Scale bar = 5 mm.

Table 5. Irritation score and irritation potential of blank nanostructured lipid carrier (Blank NLC), and nanostructured lipid carrier containing 1% *w*/*w* of Lueang Saraburi enzymatic extract (LS-EN NLC).

Samples	Irritation Score	Irritation Potential
Positive control	15.3 ± 0.3^{a}	Severe irritation
Negative control	0.0 ± 0.0^{b}	No irritation
Blank NLC	0.0 ± 0.0^{b}	No irritation
LS-EN NLC	0.0 ± 0.0^{b}	No irritation

Note: Positive control = 1% *w*/*v* sodium lauryl sulfate, negative control = 0.9% *w*/*v* sodium chloride, Blank NLC = blank nanostructured lipid carrier, and LS-EN NLC = nanostructured lipid carrier containing 1% *w*/*w* of Lueang Saraburi enzymatic extract. Values are presented as mean ± standard deviation (SD) (n = 3). Different superscript letters (a and b) within the same column indicate significant differences among samples ($p < 0.05$) according to one-way ANOVA followed by Tukey's multiple comparison test.

3.8. Release Profiles, Strat-M® Membrane Permeation, and Membrane Retention of Silk Cocoon Extract from NLCs

The in vitro release profiles of LS-EN from the solution (LS-EN SOL) and LS-EN NLC formulations are presented in Figure 6A. LS-EN SOL exhibited a rapid release, with 76 ± 1% *w*/*w* of the extract released within 24 h. In contrast, LS-EN NLC showed a significantly slower and more controlled release, reaching only 31 ± 1% *w*/*w* cumulative release over the same period, with significant differences observed at all time points ($p < 0.001$). The rapid release from the solution can be attributed to the hydrophilic nature of LS-EN, which readily diffused through the dialysis membrane into the release medium

(PBS, pH 5.5). The release medium was adjusted to pH 5.5 to mimic the mildly acidic physiological environment of the skin surface [95], thereby providing conditions relevant to topical cosmeceutical applications. In contrast, the sustained release behavior of LS-EN NLC indicates successful encapsulation of LS-EN within the lipid matrix, which acted as a diffusion barrier and modulated the release process. This controlled release is desirable for topical formulations, as it prolongs the availability of the active ingredient at the application site [96]. Mechanistically, the extract must first diffuse through or be released from the lipid nanoparticle structure before entering the surrounding medium [97], a process consistent with its high entrapment efficiency. Although conventional NLCs were originally developed primarily for hydrophobic bioactives, these results demonstrate their capability to modulate the release of hydrophilic extracts through physical entrapment within a lipid-based reservoir system [86]. The lipid matrix thereby acts as a sustained-release depot that mitigates the rapid diffusion associated with water-soluble compounds. Overall, this gradual release profile is advantageous for topical formulations, as it supports prolonged local availability of the bioactive at the application site [30,98]. However, it should be noted that the release study was based on total protein content and therefore primarily reflects the release of proteinaceous components of LS-EN. Although phenolic and flavonoid compounds may also contribute to the antioxidant activity of the extract, their release was not separately measured in this study. Further analysis of these compounds would provide a more comprehensive assessment of the antioxidant components released from the NLCs.

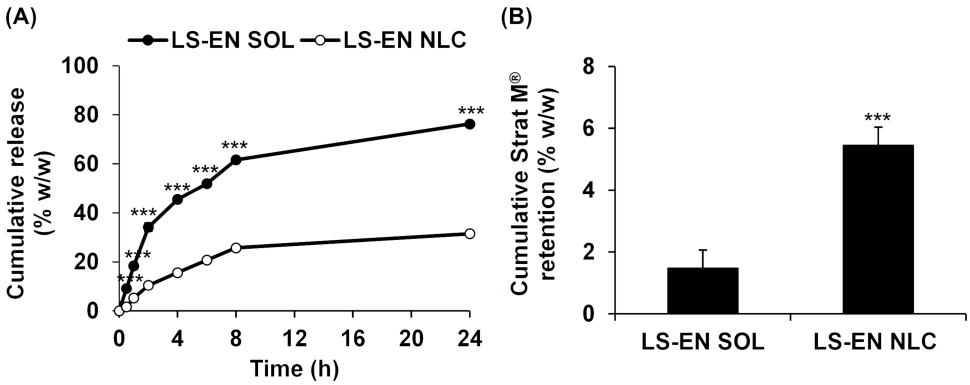


Figure 6. In vitro release (**A**) and Strat M® retention (**B**) of Lueang Saraburi enzymatic extract from solution (LS-EN SOL) and nanostructured lipid carriers (LS-EN NLC). Values are presented as mean ± standard deviation (SD) (n = 3). Asterisks indicate significant differences between LS-EN SOL and LS-EN NLC (***, $p < 0.001$).

Strat-M® membrane permeation and retention studies were subsequently performed using Franz diffusion cells. Strat-M® is a synthetic non-animal membrane designed to simulate the permeability characteristics of human skin while minimizing variability associated with biological tissues and eliminating interference from endogenous proteins during protein quantification [73,99]. It has been shown to exhibit barrier properties comparable to reconstructed human skin, particularly for hydrophilic compounds, making it a reliable surrogate for preliminary permeation studies [100]. No detectable LS-EN was found in the receptor compartment after 24 h for either the LS-EN SOL or LS-EN NLC formulation, indicating negligible permeation across the membrane. This is mainly attributed to the hydrophilic nature of LS-EN, which limits its partitioning into the lipid-associated regions of the Strat-M® structure. In addition, the membrane comprises a dense upper layer supported by progressively more porous polyether sulfone and polyolefin layers, forming a multilayered architecture that mimics the barrier function of human skin [101], thereby restricts the diffusion of highly water-soluble macromolecules. The lipid-like outer

layer further contributes to selective permeability, favoring lipophilic compounds while restricting the transport of hydrophilic proteins. Consequently, LS-EN NLC significantly increased membrane retention compared with the LS-EN SOL formulation (Figure 6B), with no detectable permeation observed ($p < 0.001$). Quantitatively, LS-EN NLC achieved a membrane retention of 5.45 ± 0.59% w/w, which was approximately 3.7-fold higher than that of the LS-EN SOL formulation (1.47 ± 0.59% w/w). This marked difference confirms the superior ability of the NLC system to localize the extract within the membrane environment. This behavior can be attributed to the nanoscale size of the lipid carriers, which increases surface contact and promotes deposition at the membrane interface [30], as well as to the lipid matrix acting as a reservoir that modulates release and diffusion [24]. Together, these properties sustain a concentration gradient that favors retention within the membrane rather than transport across it. Although Strat-M® does not fully replicate the complexity of biological skin, it remains a widely accepted and reproducible in vitro model for evaluating permeation behavior while avoiding inter-donor variability [99,101]. From a topical delivery perspective, the combination of negligible permeation and enhanced membrane retention is desirable for cosmeceutical applications, where the objective is to maintain the bioactive at the site of application rather than promote trans-barrier transport. In this context, the sustained release and localization of LS-EN from the LS-EN NLC formulation supports prolonged availability of the active compound, which is beneficial for antioxidant and anti-collagenase effects.

3.9. Facial Serum Containing Silk Cocoon Extract-Loaded NLCs

The facial serum containing silk cocoon extract-loaded NLCs exhibited a homogeneous, translucent, and viscous liquid appearance, as shown in Figure 7, both before and after centrifugation and accelerated stability testing. No visible signs of phase separation were observed, indicating good physical stability of the formulation. Following eight heating–cooling cycles, the formulation remained homogeneous with no apparent changes in visual appearance, pH, or viscosity, demonstrating satisfactory stability under accelerated storage conditions. However, the present stability assessment focused on the physical properties of the final serum, and the chemical stability of the bioactive compounds during the 28-day clinical study was not evaluated. Therefore, changes in protein and phenolic/flavonoid contents during this period could not be determined. Further chemical stability studies over the clinical treatment period, together with long-term stability studies, would provide additional information on the preservation of the bioactive compounds and support the stability of the final serum during use and storage.

As the final facial serum was developed primarily as the finished product for subsequent clinical evaluation, release and Strat-M® diffusion studies were not performed using this final serum formulation. However, these studies were conducted previously using LS-EN SOL and LS-EN NLC to directly compare the free extract with the NLC-encapsulated extract and determine the effect of NLC encapsulation on release and skin permeation. Conducting these experiments using the NLC system rather than the final serum also minimized the potential influence of other ingredients in the serum base, allowing the performance of the NLC delivery system to be evaluated more directly. The final serum was subsequently evaluated in the clinical study to determine the effect of the complete formulation on skin condition.

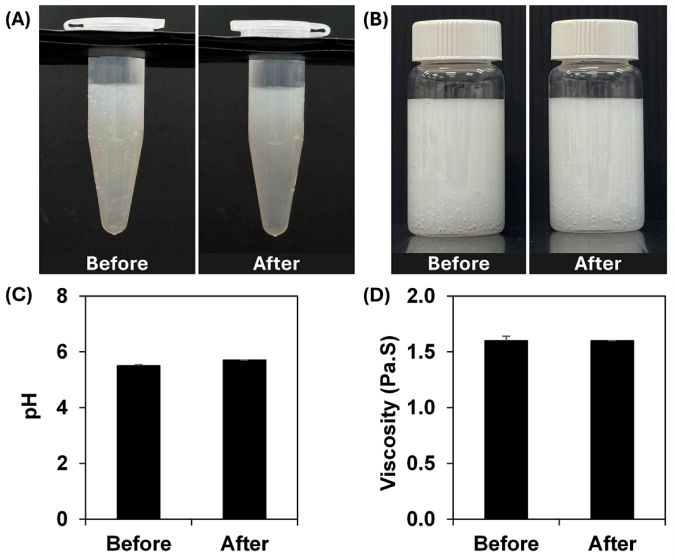


Figure 7. Visual appearance of the facial serum containing silk cocoon extract-loaded NLCs before and after centrifugation (**A**), and after accelerated stability testing involving eight heating–cooling cycles (**B**), along with the corresponding pH (**C**) and viscosity values (**D**) before and after accelerated stability testing involving eight heating–cooling cycles.

3.10. Clinical Effects of Facial Serum Containing Silk Cocoon Extract-Loaded NLCs

The results of the human skin patch test and the corresponding primary irritation potential of the facial serum containing silk cocoon extract-loaded NLCs are shown in Table 6. The findings demonstrated that the facial serum containing silk cocoon extract-loaded NLCs did not induce erythema or edema at any observation time point (4, 24, 48, or 72 h) and consequently exhibited a PII of 0, indicating no observable skin irritation. In contrast, the 20% *w*/*v* SLS positive control produced visible erythema at the assessment time points and resulted in a PII of 0.55, corresponding to slight irritation. DI water, used as the negative control, produced no erythema or edema and had a PII of 0. The visual observations shown in Figure 8 are consistent with the quantitative patch test results. The application site of the facial serum showed no apparent erythematous response or edema throughout the observation period, whereas the SLS-treated site demonstrated visible skin changes following application. The absence of visible irritation at the serum-treated site, together with the absence of measurable erythema and edema, supports the good skin tolerability and no irritation potential of the facial serum.

Table 6. Human skin patch test and primary irritation potential of the facial serum containing silk cocoon extract-loaded NLCs.

Sample	Erythema Formation Score				Edema Formation Score				PII	Irritation Potential
	4 h	24 h	48 h	72 h	4 h	24 h	48 h	72 h		
20% *w*/*v* SLS	0	26	24	20	0	0	0	0	0.55	Slightly irritation
DI water	0	0	0	0	0	0	0	0	0	No irritation
Facial serum containing silk cocoon extract-loaded NLCs	0	0	0	0	0	0	0	0	0	No irritation

Note: 20% *w*/*v* Sodium lauryl sulfate (SLS) was used as positive control; DI water was used negative control; PII = primary irritation index (n = 30).

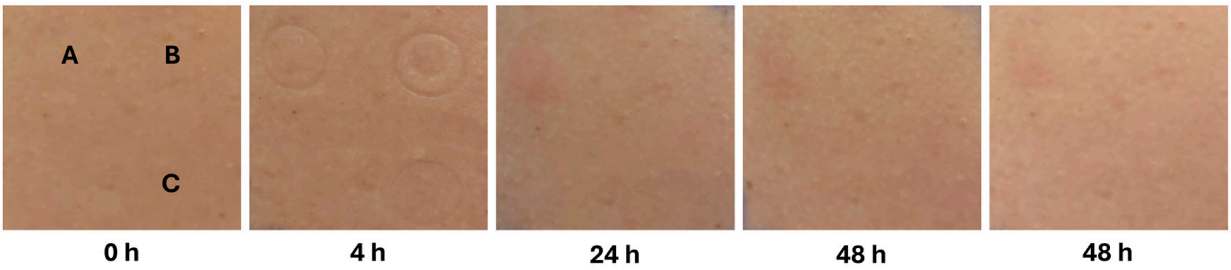


Figure 8. Representative images of the outer aspect of a volunteer's left upper arm showing the application sites for the patch test: (A) 20% w/v sodium lauryl sulfate (SLS), (B) DI water, and (C) facial serum containing silk cocoon extract-loaded NLCs, captured before application (0 h) and after 4, 24, 48, and 72 h of patch application (n = 30).

The effects of the facial serum containing silk cocoon extract-loaded NLCs on skin moisture and wrinkles were evaluated over a 28-day treatment period using a Corneometer® and Visioscan®, respectively. As shown in Table 7, Corneometer® measurements revealed a progressive increasing trend in skin moisture throughout the treatment period. The skin moisture increased by 1.43%, 5.58%, and 7.05% after 7, 14, and 28 days, respectively. Although the observed changes were not statistically significant, skin moisture increased gradually from baseline to day 28. The findings also indicated that repeated application of the facial serum improved the hydration status of the facial skin. The improvement may be attributed to the occlusive and moisturizing properties of the NLC-based delivery system, which can promote moisture retention and reduce transepidermal water loss [30]. In addition, the silk cocoon extract may contribute to the skin-conditioning properties of the formulation, as previous research demonstrated that silkworm cocoon extracts significantly enhanced skin moisture, supporting their potential application as moisturizing cosmetic ingredients [14].

Table 7. Effects of topical application of the facial serum containing silk cocoon extract-loaded NLCs on skin hydration and skin surface roughness at baseline (Day 0) and after 7, 14, and 28 days of treatment.

Skin Parameter	Baseline	Day 7	Day 14	Day 28
Skin Hydration	61.35 ± 17.20	62.22 ± 13.75 (+1.43%)	64.77 ± 14.24 (+5.58%)	65.67 ± 13.47 (+7.05%)
Average Roughness	31.31 ± 3.67	30.92 ± 3.01 (−1.26%)	31.60 ± 3.01 (+0.93%)	29.03 ± 3.40 * (−7.29%)
Arithmetic average roughness	6.65 ± 0.77	6.80 ± 0.71 (+2.35%)	6.79 ± 0.82 (+2.19%)	6.20 ± 0.77 * (−6.74%)

Note: Data are presented as mean ± standard deviation (SD), with percentage changes from baseline shown in parentheses. Asterisk (*) indicates a statistically significant difference compared with baseline (n = 30).

Importantly, the findings revealed a reduction in both average roughness and arithmetic roughness after 28 days of treatment, as shown in Table 7. The findings indicated an improvement in skin surface microtopography and smoothness. Average roughness represents the mean variation in grayscale intensity within wrinkle regions of a two-dimensional skin image, providing an estimate of overall surface irregularity [102], whereas arithmetic mean roughness represents the average magnitude of surface deviations across the analyzed skin area, providing an overall measure of surface roughness and heterogeneity [103]. Both average roughness and arithmetic roughness significantly decreased by 7.29% and

6.74%, respectively, compared with baseline ($p < 0.05$). Although slight fluctuations were observed during the first 14 days, the reduction observed on day 28 indicated an overall improvement in skin surface smoothness following continuous application of the facial serum. Representative Visioscan® images in Figure 9 also support these findings, showing a visible progressive improvement in skin surface appearance, with a reduction in the prominence of fine surface lines and a smoother, more uniform skin microtopography by day 28 compared with baseline. This visual improvement is consistent with the instrumental reduction in average and arithmetic roughness (Table 7), further supporting the potential of the facial serum to improve skin surface smoothness and reduce the appearance of wrinkles following continuous treatment. However, it should be noted that the clinical evaluation was conducted as a baseline-controlled study without a placebo or vehicle-controlled formulation. Therefore, the observed improvements may have resulted from the overall formulation and the combined effects of its various components, rather than being attributable solely to the LS-EN NLCs. The improvement effects could be associated with the serum base formulation, the NLC base formulation, repeated application, or other confounding factors that cannot be excluded, particularly for skin moisture, which may be influenced by the base formulations. Nevertheless, the findings provide clinical evidence supporting the potential benefits of the final serum formulation for skin condition. Further placebo- or vehicle-controlled studies are suggested to clarify the specific contribution of LS-EN NLC to the observed effects.

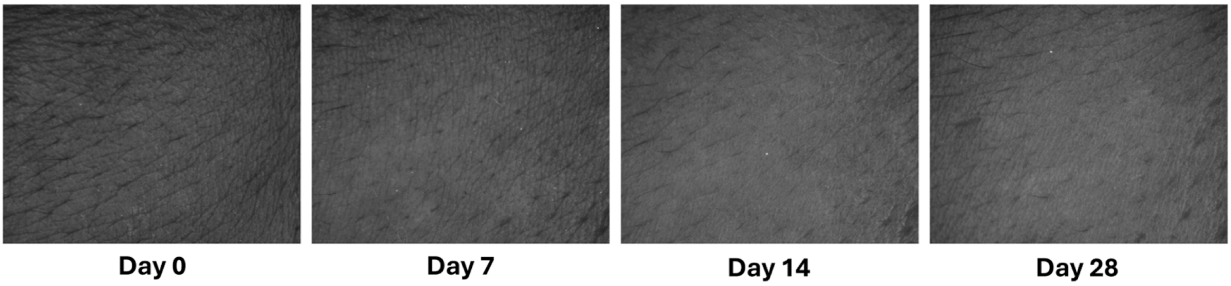


Figure 9. Representative Visioscan® images showing changes in skin surface following topical application of the facial serum containing silk cocoon extract-loaded NLCs at baseline (Day 0) and after 7, 14, and 28 days of treatment ($n = 30$).

The satisfaction scores presented in Table 8 demonstrate that the respondents reported a high level of satisfaction with all aspects evaluated. The facial serum containing silk cocoon extract-loaded NLCs was particularly well received for its homogeneous appearance and skin compatibility, with favorable perceptions of its texture, spreadability, absorption, and ability to leave the skin feeling soft, smooth, and silky. The product's visual and sensory characteristics, including its color, viscosity, and fragrance, were also positively evaluated. Regarding skin improvement benefits, respondents perceived the product as beneficial for enhancing skin hydration, improving overall skin appearance, and addressing concerns such as wrinkles, dullness, enlarged pores, and dark spots. Therefore, the findings indicate that the product was well accepted by the respondents and provided a satisfactory user experience in terms of appearance, sensory properties, and perceived skin benefits.

Table 8. Satisfaction scores for the facial serum containing silk cocoon extract-loaded NLCs.

Details	Mean Satisfaction Score	Satisfaction Level
Product visual appearance		
Homogeneous appearance	4.34 ± 0.75	High
Appropriate viscosity	3.91 ± 1.12	High
Appealing color	4.09 ± 0.86	High
Pleasant fragrance	3.94 ± 1.11	High
Sensory performance		
Non-sticky and non-greasy feel	4.00 ± 0.88	High
Spreads easily on the skin	4.19 ± 0.90	High
Absorbs well into the skin	4.19 ± 0.74	High
Does not cause allergic reactions or skin irritation	4.34 ± 0.79	High
Makes the skin soft and smooth	4.13 ± 0.83	High
Provides a smooth and silky skin feel	4.06 ± 0.84	High
Skin improvement benefits		
Reduces the appearance of wrinkles	3.81 ± 0.69	High
Brightens the skin	3.78 ± 0.79	High
Improves skin hydration	4.13 ± 0.71	High
Makes pores appear less visible	3.69 ± 0.86	High
Reduces the appearance of dark spots	3.72 ± 0.92	High
Overall satisfaction with the product	4.09 ± 0.93	High

Note: Data are presented as mean ± standard deviation (SD) (n = 30).

4. Conclusions

The recovery of bioactive constituents from *B. mori* silk cocoons was strongly influenced by both silkworm strain and the extraction method, with enzymatic extraction of the LS strain producing the most promising extract in terms of chemical composition, antioxidant and collagenase inhibitory activities, and non-irritating safety profile. Incorporation of LS-EN into NLCs resulted in a physically stable formulation with high entrapment efficiency and successfully modulated the release of the hydrophilic extract, providing sustained release and enhanced localization within the Strat-M® membrane. Notably, the LS-EN NLC formulation increased membrane retention by approximately 3.7-fold compared with the LS-EN SOL while exhibiting negligible permeation across the membrane, indicating that the delivery system effectively retained the bioactive at the application site rather than promoting transdermal transport. This localized delivery profile is particularly advantageous for topical cosmeceutical applications, where prolonged residence of the active ingredient within the skin can maximize antioxidant and anti-collagenase activities while minimizing unnecessary systemic exposure. Furthermore, the LS-EN-loaded NLC facial serum showed good physical stability and skin tolerability, with no observable ir-

ritation. After 28 days, skin moisture increased by 7.05%, while average and arithmetic roughness significantly decreased by 7.29% and 6.74%, respectively ($p < 0.05$). Together with the 3.7-fold higher membrane retention and negligible permeation, these findings support its potential as a safe and effective localized delivery system for anti-aging cosmeceutical applications. Additionally, the LS-EN-loaded NLC facial serum demonstrated high overall consumer satisfaction, with favorable acceptance across its physical appearance, sensory attributes, skin tolerability, and perceived skin-enhancing benefits, further supporting its potential for use in anti-aging cosmeceutical applications.

Author Contributions: Conceptualization, W.C.; methodology, S.C. and W.C.; validation, S.C. and W.C.; formal analysis, S.C.; investigation, S.C.; resources, W.C.; data curation, W.C.; writing—original draft preparation, S.C. and W.C.; writing—review and editing, S.C. and W.C.; visualization, W.C.; supervision, W.C.; project administration, W.C.; funding acquisition, S.C. and W.C. All authors have read and agreed to the published version of the manuscript.

Funding: This research was funded by the Fundamental Fund 2026, Chiang Mai University. Sarocha Chareegun expresses sincere gratitude for the Teaching Assistant and Research Assistant (TA/RA) scholarship provided by Chiang Mai University and the Research and Researchers for Industry (RRI) Program by National Research Council of Thailand (NRCT), grant number N23G690007. This research was also funded by Chiang Mai University, Chiang Mai, Thailand, and the Center of Excellence in Pharmaceutical Nanotechnology, Faculty of Pharmacy, Chiang Mai University, Chiang Mai, Thailand.

Institutional Review Board Statement: As this study does not involve human subjects, Institutional Review Board approval is not applicable.

Informed Consent Statement: Not applicable.

Data Availability Statement: The original contributions presented in this study are included in the article. Further inquiries can be directed at the corresponding author.

Acknowledgments: The authors would like to acknowledge the Queen Sirikit Sericulture Center, Chiang Mai, Thailand, for their generous support in providing the silkworm cocoon materials. GPT-5.3-mini (OpenAI), San Francisco, CA, USA (https://openai.com), was used for grammar correction and reference formatting. All authors carefully reviewed and approved the edited text and accepted full responsibility for the final version of the manuscript.

Conflicts of Interest: The authors declare no conflicts of interest.

Abbreviations

The following abbreviations are used in this manuscript:

ABTS	2,2′-Azino-bis(3-ethylbenzothiazoline-6-sulfonic acid)
ANOVA	Analysis of variance
AQ	Aqueous extraction
ASC	Ascorbic acid
BCA	Bicinchoninic acid
BSA	Bovine serum albumin
CAM	Chorioallantoic membrane
DI	Deionized
DLS	Dynamic light scattering
DPPH	2,2-Diphenyl-1-picrylhydrazyl
EC_1	Equivalent concentration
EDTA	Ethylenediaminetetraacetic acid
EGCG	Epigallocatechin gallate
EN	Enzyme-assisted extraction
FALGPA	N-[3-(2-Furyl)acryloyl]-Leu-Gly-Pro-Ala

FRAP	Ferric reducing antioxidant power
GAE	Gallic acid equivalent
GAL	Gallic acid
GMS	Glyceryl monostearate
HET-CAM	Hen's egg test on chorioallantoic membrane
IC_{50}	Half-maximal inhibitory concentration
IS	Irritation score
LS	Lueang Saraburi
LS-AQ	Lueang Saraburi aqueous extract
LS-EN	Lueang Saraburi enzymatic extract
MMP-1	Matrix metalloproteinase-1
MWCO	Molecular weight cut-off
NL	Nang Lai
NL-AQ	Nang Lai aqueous extract
NL-EN	Nang Lai enzymatic extract
NLC	Nanostructured lipid carrier
NS	Not significant
NSS	Normal saline solution
PBS	Phosphate-buffered saline
PDI	Polydispersity index
PII	Primary irritation index
QE	Quercetin equivalent
SD	Standard deviation
SER	Standard sericin
SLS	Sodium lauryl sulfate
TEM	Transmission electron microscopy
TFC	Total flavonoid content
TPC	Total phenolic content
TPTZ	2,4,6-Tripyridyl-s-triazine

References

1. Silva, A.S.; Costa, E.C.; Reis, S.; Spencer, C.; Calhelha, R.C.; Miguel, S.P.; Ribeiro, M.P.; Barros, L.; Vaz, J.A.; Coutinho, P. Silk sericin: A promising sustainable biomaterial for biomedical and pharmaceutical applications. *Polymers* **2022**, *14*, 4931. [CrossRef] [PubMed]
2. Biganeh, H.; Kabiri, M.; Zeynalpourfattahi, Y.; Brancalhão, R.M.C.; Karimi, M.; Shams Ardekani, M.R.; Rahimi, R. *Bombyx mori* cocoon as a promising pharmacological agent: A review of ethnopharmacology, chemistry, and biological activities. *Heliyon* **2022**, *8*, e10496. [CrossRef] [PubMed]
3. Krongdang, S.; Phokasem, P.; Venkatachalam, K.; Charoenphun, N. Edible insects in Thailand: An overview of status, properties, processing, and utilization in the food industry. *Foods* **2023**, *12*, 2162. [CrossRef] [PubMed]
4. Suresh, G.; Saha, D.; Kumari, A.; Palsaniya, M.; Garhwal, P.C.; Singh, V.P.; Dadrwal, B.K. Mulberry leaf metabolomics: Linking plant biochemistry with silkworm physiology and sustainable sericulture. *J. Adv. Biol. Biotechnol.* **2026**, *29*, 57–80. [CrossRef]
5. Guo, H.; Sun, Y.; Shi, W.; Huang, R.; He, Q.; Zhao, P.; Xia, Q. Novel GS5 sericin mitigates UVA-induced photoaging by activating Nrf2 and inhibiting the JAK-STAT pathway. *Int. J. Biol. Sci.* **2026**, *22*, 1496. [CrossRef] [PubMed]
6. Guo, X.; He, L.; Sun, J.; Ye, H.; Yin, C.; Zhang, W.; Han, H.; Jin, W. Exploring the potential of anthocyanins for repairing photoaged skin: A comprehensive review. *Foods* **2024**, *13*, 3506. [CrossRef] [PubMed]
7. Siritientong, T.; Bonani, W.; Motta, A.; Migliaresi, C.; Aramwit, P. The effects of Bombyx mori silk strain and extraction time on the molecular and biological characteristics of sericin. *Biosci. Biotechnol. Biochem.* **2016**, *80*, 241–249. [CrossRef] [PubMed]
8. Kunz, R.I.; Brancalhão, R.M.C.; Ribeiro, L.D.F.C.; Natali, M.R.M. Silkworm sericin: Properties and biomedical applications. *BioMed Res. Int.* **2016**, *2016*, 8175701. [CrossRef] [PubMed]
9. Wang, Y.; Gao, J.; Yang, Y.; Zhu, L.; Yang, W.; Li, P.; Yang, W. A review on the extraction methods, bioactivities, and application in foods of silk sericin. *J. Food Biochem.* **2025**, *2025*, 2155701. [CrossRef]
10. Aad, R.; Dragojlov, I.; Vesentini, S. Sericin protein: Structure, properties, and applications. *J. Funct. Biomater.* **2024**, *15*, 322. [CrossRef] [PubMed]

11. Kabir, M.; Hasan, M.K.; Rafi, M.N.; Repon, M.R.; Islam, T.; Saha, J.; Rahman, M. Biowaste transformation to functional materials: Structural properties, extraction methods, applications, and challenges of silk sericin. *ChemistrySelect* **2024**, *9*, e202403777. [CrossRef]
12. Wang, H.Y.; Wang, Y.J.; Zhou, L.X.; Zhu, L.; Zhang, Y.Q. Isolation and bioactivities of a non-sericin component from cocoon shell silk sericin of the silkworm *Bombyx mori*. *Food Funct.* **2012**, *3*, 150–158. [CrossRef] [PubMed]
13. Wu, J.H.; Wang, Z.; Xu, S.Y. Enzymatic production of bioactive peptides from sericin recovered from silk industry wastewater. *Process Biochem.* **2008**, *43*, 480–487. [CrossRef]
14. Chareegun, S.; Somwongin, S.; Inthorn, J.; Juntrapirom, S.; Kanjanakawinkul, W.; Chaiyana, W. Comparative effects of microwave and ultrasonic pretreatments on the antioxidant, anti-aging, and moisturizing activities of yellow silkworm cocoon extracts (*Bombyx mori* L., var. Nang Lai). *Cosmetics* **2025**, *12*, 170. [CrossRef]
15. Chieco, C.; Morrone, L.; Bertazza, G.; Cappellozza, S.; Saviane, A.; Gai, F.; Di Virgilio, N.; Rossi, F. The effect of strain and rearing medium on the chemical composition, fatty acid profile and carotenoid content in silkworm (*Bombyx mori*) pupae. *Animals* **2019**, *9*, 103. [CrossRef] [PubMed]
16. Sivaprasad, V.; Chandrakanth, N.; Moorthy, S.M. Genetics and genomics of *Bombyx mori* L. In *Genetic Methods and Tools for Managing Crop Pests*; Chakravarthy, A.K., Ed.; Springer: Singapore, 2022; pp. 123–146. [CrossRef]
17. Kampapongsa, D.; Promma, S.; Sumida, M.; Nianwithu, K. Effect of young and mature coconut water on cocoon characters of Thai polyvoltine strains, Nang-Noi and Nang-Lai, of the silkworm, *Bombyx mori*. *Int. J. Wild Silkmoth Silk* **2017**, *20*, 17–23. [CrossRef] [PubMed]
18. Homhuk, P.; Nonsrirach, T.; Promma, S.; Sumida, M.; Sutthikhum, V. Cocoon characters and antioxidant activity of sericin among Thai polyvoltine strains of the silkworm, Bombyx mori. *Int. J. Wild Silkmoth Silk* **2017**, *20*, 25–36. [CrossRef] [PubMed]
19. Trommer, H.; Neubert, R.H.H. Overcoming the stratum corneum: The modulation of skin penetration: A review. *Ski. Pharmacol. Physiol.* **2006**, *19*, 106–121. [CrossRef] [PubMed]
20. Jeong, W.Y.; Kwon, M.; Choi, H.E.; Kim, K.S. Recent advances in transdermal drug delivery systems: A review. *Biomater. Res.* **2021**, *25*, 24. [CrossRef] [PubMed]
21. Akombaetwa, N.; Ilangala, A.B.; Thom, L.; Memvanga, P.B.; Witika, B.A.; Buya, A.B. Current advances in lipid nanosystems intended for topical and transdermal drug delivery applications. *Pharmaceutics* **2023**, *15*, 656. [CrossRef]
22. Chen, Y.; Feng, X.; Meng, S. Site-specific drug delivery in the skin for the localized treatment of skin diseases. *Expert Opin. Drug Deliv.* **2019**, *16*, 847–867. [CrossRef]
23. Khan, S.; Sharma, A.; Jain, V. An overview of nanostructured lipid carriers and its application in drug delivery through different routes. *Adv. Pharm. Bull.* **2023**, *13*, 446. [CrossRef] [PubMed]
24. Souto, E.B.; Fangueiro, J.F.; Fernandes, A.R.; Cano, A.; Sanchez-Lopez, E.; Garcia, M.L.; Severino, P.; Paganelli, M.O.; Chaud, M.V.; Silva, A.M. Physicochemical and biopharmaceutical aspects influencing skin permeation and role of SLN and NLC for skin drug delivery. *Heliyon* **2022**, *8*, e08938. [CrossRef] [PubMed]
25. Fitriani, E.W.; Avanti, C.; Rosana, Y.; Surini, S. Nanostructured lipid carriers: A prospective dermal drug delivery system for natural active ingredients. *Pharmacia* **2024**, *71*, 1–15. [CrossRef]
26. Kothapalli, P.; Vasanthan, M. Lipid-based nanocarriers for enhanced delivery of plant-derived bioactive molecules: A comprehensive review. *Ther. Deliv.* **2024**, *15*, 135–155. [CrossRef]
27. Nurohman, I.; Suhandi, C.; Chaerunisaa, A.Y.; Wilar, G.; Jafar, G.; Sriwidodo, S. Design evolution of curcumin-loaded nanostructured lipid carriers: Formulation strategies, functional modifications, and mechanistic–translational perspectives. *Int. J. Nanomed.* **2026**, *21*, 586727. [CrossRef]
28. Boskabadi, M.; Saeedi, M.; Akbari, J.; Morteza-Semnani, K.; Hashemi, S.M.H.; Babaei, A. Topical gel of vitamin A solid lipid nanoparticles: A hopeful promise as a dermal delivery system. *Adv. Pharm. Bull.* **2021**, *11*, 663. [CrossRef] [PubMed]
29. Parida, G.K.; Mohapatra, S.; Kar, R.K. Solid lipid nanoparticles: A new approach of colloidal drug carrier. *World J. Pharm. Pharm. Sci.* **2016**, *5*, 2124–2142.
30. Alquraisy, A.; Ramadhani, K.; Mohammed, A.F.A.; Wilar, G.; Osman, W.; Elamin, K.M.; Wathoni, N. Nanostructured lipid carrier-gels for wound healing: A narrative review of formulation strategies, mechanisms, and translational potential. *Nanotechnol. Sci. Appl.* **2026**, *19*, 585159. [CrossRef] [PubMed]
31. Sharma, G.; Thakur, K.; Raza, K.; Singh, B.; Katare, O.P. Nanostructured lipid carriers: A new paradigm in topical delivery for dermal and transdermal applications. *Crit. Rev. Ther. Drug Carr. Syst.* **2017**, *34*, 355–386. [CrossRef] [PubMed]
32. Bungthong, C.; Siriamornpun, S. Changes in amino acid profiles and bioactive compounds of Thai silk cocoons as affected by water extraction. *Molecules* **2021**, *26*, 2033. [CrossRef] [PubMed]
33. Shea, F.; Watts, C.E. Dumas method for organic nitrogen. *Ind. Eng. Chem. Anal. Ed.* **1939**, *11*, 333–334. [CrossRef]
34. Choi, B.D.; Wong, N.A.K.; Auh, J.H. Defatting and sonication enhances protein extraction from edible insects. *Korean J. Food Sci. Anim. Resour.* **2017**, *37*, 955–961. [CrossRef] [PubMed]

35. Maehre, H.K.; Dalheim, L.; Edvinsen, G.K.; Elvevoll, E.O.; Jensen, I.J. Protein determination—Method matters. *Foods* **2018**, *7*, 5. [CrossRef] [PubMed]
36. Brown, R.E.; Jarvis, K.L.; Hyland, K.J. Protein measurement using bicinchoninic acid: Elimination of interfering substances. *Anal. Biochem.* **1989**, *180*, 136–139. [CrossRef] [PubMed]
37. Singleton, V.L.; Orthofer, R.; Lamuela-Raventós, R.M. Analysis of total phenols and other oxidation substrates and antioxidants by means of Folin-Ciocalteu reagent. *Methods Enzymol.* **1999**, *299*, 152–178. [CrossRef]
38. Chang, C.C.; Yang, M.H.; Wen, H.M.; Chern, J.C. Estimation of total flavonoid content in propolis by two complementary colorimetric methods. *J. Food Drug Anal.* **2002**, *10*, 178–182. [CrossRef]
39. Brand-Williams, W.; Cuvelier, M.E.; Berset, C. Use of a free radical method to evaluate antioxidant activity. *LWT-Food Sci. Technol.* **1995**, *28*, 25–30. [CrossRef]
40. Re, R.; Pellegrini, N.; Proteggente, A.; Pannala, A.; Yang, M.; Rice-Evans, C. Antioxidant activity applying an improved ABTS radical cation decolorization assay. *Free Radic. Biol. Med.* **1999**, *26*, 1231–1237. [CrossRef] [PubMed]
41. Benzie, I.F.F.; Strain, J.J. The ferric reducing ability of plasma (FRAP) as a measure of "antioxidant power": The FRAP assay. *Anal. Biochem.* **1996**, *239*, 70–76. [CrossRef] [PubMed]
42. Thring, T.S.A.; Hili, P.; Naughton, D.P. Anti-collagenase, anti-elastase and anti-oxidant activities of extracts from 21 plants. *BMC Complement. Altern. Med.* **2009**, *9*, 27. [CrossRef] [PubMed]
43. Luepke, N.P. Hen's egg chorioallantoic membrane test for irritation potential. *Food Chem. Toxicol.* **1985**, *23*, 287–291. [CrossRef] [PubMed]
44. Freire, P.L.; Stamford, T.C.M.; Albuquerque, A.J.; Sampaio, F.C.; Cavalcante, H.M.; Macedo, R.O.; Galembeck, A.; Flores, M.A.; Rosenblatt, A. Action of silver nanoparticles towards biological systems: Cytotoxicity evaluation using hen's egg test and inhibition of Streptococcus mutans biofilm formation. *Int. J. Antimicrob. Agents* **2015**, *45*, 183–187. [CrossRef] [PubMed]
45. Shirazi, A.S.; Varshochian, R.; Rezaei, M.; Ardakani, Y.H.; Dinarvand, R. SN38 loaded nanostructured lipid carriers (NLCs); preparation and in vitro evaluations against glioblastoma. *J. Mater. Sci. Mater. Med.* **2021**, *32*, 78. [CrossRef] [PubMed]
46. Carpenter, J.; Saharan, V.K. Ultrasonic assisted formation and stability of mustard oil in water nanoemulsion: Effect of process parameters and their optimization. *Ultrason. Sonochem.* **2017**, *35*, 422–430. [CrossRef] [PubMed]
47. Rosli, N.A.; Hasham, R.; Aziz, A.A.; Noh, T.U.; Jemon, K. Nanostructured lipid carrier loaded with *Zingiber officinale* oil to enhance transdermal bioactive delivery for topical formulation. *Microchem. J.* **2024**, *200*, 110470. [CrossRef]
48. Garg, N.K.; Tandel, N.; Bhadada, S.K.; Tyagi, R.K. Nanostructured lipid carrier–mediated transdermal delivery of aceclofenac hydrogel present an effective therapeutic approach for inflammatory diseases. *Front. Pharmacol.* **2021**, *12*, 713616. [CrossRef] [PubMed]
49. Arce, F.J.; Asano, N.; See, G.L.; Itakura, S.; Todo, H.; Sugibayashi, K. Usefulness of artificial membrane, Strat-M®, in the assessment of drug permeation from complex vehicles in finite dose conditions. *Pharmaceutics* **2020**, *12*, 173. [CrossRef] [PubMed]
50. Simon, A.; Amaro, M.I.; Healy, A.M.; Cabral, L.M.; de Sousa, V.P. Comparative evaluation of rivastigmine permeation from a transdermal system in the Franz cell using synthetic membranes and pig ear skin with in vivo-in vitro correlation. *Int. J. Pharm.* **2016**, *512*, 234–241. [CrossRef] [PubMed]
51. Yeerong, K.; Czyrski, G.S.; Heinz, A.; Müllertz, A.; Rades, T.; Chaiyana, W. Transdermal delivery of *Acheta domesticus* protein hydrolysate using nanostructured lipid carriers and Derma Stamp—Does the combination of lipid-based formulation and a physical technique add value for permeation and retention? *J. Drug Deliv. Sci. Technol.* **2025**, *104*, 106470. [CrossRef]
52. Pellevoisin, C.; Coleman, K.P.; Hoffmann, S. ISO 10993-23 In vitro irritation testing for medical devices: Substantiating applicability to mild irritants and non-extractables. *Toxicol. In Vitro* **2022**, *82*, 105371. [CrossRef] [PubMed]
53. Bagley, D.M.; Gardner, J.R.; Holland, G.; Lewis, R.W.; Régnier, J.F.; Stringer, D.A.; Walker, A.P. Skin irritation: Reference chemicals data bank. *Toxicol. In Vitro* **1996**, *10*, 1–6. [CrossRef] [PubMed]
54. Joshi, A.; Kale, S.; Chandel, S.; Pal, D.K. Likert scale: Explored and explained. *Br. J. Appl. Sci. Technol.* **2015**, *7*, 396–403. [CrossRef]
55. Magnussen, K.; Promma, S. A preliminary study of juvenile hormone analogue, pyriproxyfen, on growth and economic characters of Thai hybrid silkworm, *Bombyx mori* L. (Nanglai × J108 strain) by topical application. *Int. J. Wild Silkmoth Silk* **2015**, *19*, 37–44. [CrossRef] [PubMed]
56. Soomherun, N.; Thongchai, K.; Chimma, A.; Keeratihattayakorn, S.; Ratanavaraporn, J. Comparative study of yellow *Bombyx mori* cocoons for development of an injectable silk fibroin hydrogel as drug delivery system. *Mater. Today Chem.* **2025**, *47*, 102856. [CrossRef]
57. Pitjamit, S.; Thunsiri, K.; Nakkiew, W.; Pothacharoen, P. Preparation and characterization of silk fibroin from four different species of Thai-local silk cocoon for bone implant applications. *IOP Conf. Ser. Mater. Sci. Eng.* **2019**, *635*, 012001. [CrossRef]
58. Liu, S.; Zhang, Q.; Zhou, H.; Zhang, B.; Yu, M.; Wang, Y.; Liu, Y.; Chai, C. The potential of natural carotenoids-containing sericin of the domestic silkworm Bombyx mori. *Int. J. Mol. Sci.* **2024**, *25*, 3688. [CrossRef] [PubMed]
59. Joseph, Z.; Ishay, J.S. Silk structure in the hornet cocoon. *Microscopy* **2004**, *53*, 293–304. [CrossRef] [PubMed]

60. Suraporn, S.; Sangsuk, W.; Chanhan, P.; Promma, S. Effects of probiotic bacteria on the growth parameters of the Thai silkworm, Bombyx mori. *Thai J. Agric. Sci.* **2015**, *48*, 29–33.
61. Sumriddetchkajorn, S.; Kamtongdee, C.; Chanhorm, S. Fault-tolerant optical-penetration-based silkworm gender identification. *Comput. Electron. Agric.* **2015**, *119*, 201–208. [CrossRef]
62. Gulrajani, M.L. Degumming of silk. In *Silk Dyeing, Printing and Finishing*; Gulrajani, M.L., Ed.; Department of Textile Technology, Indian Institute of Technology: New Delhi, India, 1988; pp. 63–95.
63. Kurioka, A.; Yamazaki, M. Purification and identification of flavonoids from the yellow-green cocoon shell (Sasamayu) of the silkworm, Bombyx mori. *Biosci. Biotechnol. Biochem.* **2002**, *66*, 1396–1399. [CrossRef] [PubMed]
64. Paavana, O.S.K.; Sruthi, S.P.; Patel, M.; Karthik, M.G.; Nair, V.R.; Nadar, M. From cocoons to cures: The emerging role of Bombyx mori silk proteins in pharmacological research. *Curr. Pharmacol. Rep.* **2026**, *12*, 6. [CrossRef]
65. Gulrajani, M.L. Degumming of silk. *Rev. Prog. Color. Relat. Top.* **1992**, *22*, 79–89. [CrossRef]
66. Walker, J.M. The bicinchoninic acid (BCA) assay for protein quantitation. In *The Protein Protocols Handbook*; Walker, J.M., Ed.; Springer Protocols Handbooks; Humana Press: Totowa, NJ, USA, 2009. [CrossRef]
67. Joseph, P.S.; Selvasudha, N.; Meenakshi, D.U.; Ganesan, P.; Thekkila-Veedu, S.; Mohanan, D.P.; George, A.M.; Kandasamy, R. Pharmaceutical, therapeutic, and cosmetic applications of sericin. In *Biopolymers in Pharmaceutical and Food Applications*; Wiley: Hoboken, NJ, USA, 2024; pp. 641–670. [CrossRef]
68. Seo, S.J.; Das, G.; Shin, H.S.; Patra, J.K. Silk sericin protein materials: Characteristics and applications in food-sector industries. *Int. J. Mol. Sci.* **2023**, *24*, 4951. [CrossRef] [PubMed]
69. Zhao, J.G.; Zhang, Y.Q. A new estimation of the total flavonoids in silkworm cocoon sericin layer through aglycone determination by hydrolysis-assisted extraction and HPLC-DAD analysis. *Food Nutr. Res.* **2016**, *60*, 30932. [CrossRef] [PubMed]
70. Urbanek Krajnc, A.; Bakonyi, T.; Ando, I.; Kurucz, E.; Solymosi, N.; Pongrac, P.; Berčič, R.L. The effect of feeding with Central European local mulberry genotypes on the development and health status of silkworms and quality parameters of raw silk. *Insects* **2022**, *13*, 836. [CrossRef] [PubMed]
71. Waizumi, R.; Hirayama, C.; Tomita, S.; Iizuka, T.; Kuwazaki, S.; Jouraku, A.; Tsubota, T.; Yokoi, K.; Yamamoto, K.; Sezutsu, H. A major endogenous glycoside hydrolase mediating quercetin uptake in Bombyx mori. *PLoS Genet.* **2024**, *20*, e1011118. [CrossRef] [PubMed]
72. Kanyora, M.G.; Kegode, T.M.; Kurgat, J.; Kibogo, H.; Asudi, G.; Tanga, C.M.; Ayalew, W.; Sevgan, S.; Ndungu, N. Evaluating antibacterial and antioxidant properties of sericin recovered from cocoons of *Bombyx mori*, *Gonometa postica* and *Samia ricini* in Kenya. *PLoS ONE* **2024**, *19*, e0316259. [CrossRef] [PubMed]
73. Gordon, S.; Daneshian, M.; Bouwstra, J.; Caloni, F.; Constant, S.; Davies, D.E.; Dandekar, G.; Guzman, C.A.; Fabian, E.; Haltner, E.; et al. Non-animal models of epithelial barriers (skin, intestine and lung) in research, industrial applications and regulatory toxicology. *ALTEX* **2015**, *32*, 327–378. [CrossRef] [PubMed]
74. Gulcin, İ. Antioxidants: A comprehensive review. *Arch. Toxicol.* **2025**, *99*, 1893–1997. [CrossRef] [PubMed]
75. Lai, C.F.; Esam, G.; Lin, Y.C.; Chung, R.J. From destruction to protection: Rethinking MMP-1 in skin aging and anti-aging strategies. *Arch. Dermatol. Res.* **2026**, *318*, 56. [CrossRef]
76. Feng, C.; Chen, X.; Yin, X.; Jiang, Y.; Zhao, C. Matrix metalloproteinases on skin photoaging. *J. Cosmet. Dermatol.* **2024**, *23*, 3847–3862. [CrossRef] [PubMed]
77. Quan, T.; Fisher, G.J. Role of age-associated alterations of the dermal extracellular matrix microenvironment in human skin aging: A mini-review. *Gerontology* **2015**, *61*, 427–434. [CrossRef] [PubMed]
78. Leopoldini, M.; Marino, T.; Russo, N.; Toscano, M. Antioxidant properties of phenolic compounds: H-atom versus electron transfer mechanism. *J. Phys. Chem. A* **2004**, *108*, 4916–4922. [CrossRef]
79. Pietta, P.G. Flavonoids as antioxidants. *J. Nat. Prod.* **2000**, *63*, 1035–1042. [CrossRef] [PubMed]
80. Steiling, W.; Bracher, M.; Courtellemont, P.; De Silva, O. The HET–CAM, a useful in vitro assay for assessing the eye irritation properties of cosmetic formulations and ingredients. *Toxicol. In Vitro* **1999**, *13*, 375–384. [CrossRef] [PubMed]
81. de Silva, O.; Rougier, A.; Dossou, K.G. The HET-CAM test: A study of the irritation potential of chemicals and formulations. *Altern. Lab. Anim.* **1992**, *20*, 432–437. [CrossRef]
82. Wang, F.; Zhang, C.; Wang, B. Application of in vitro methods to evaluate the safety of baby care products. *Toxicol. In Vitro* **2021**, *75*, 105194. [CrossRef] [PubMed]
83. Sandner, G.; König, A.; Wallner, M.; Weghuber, J. Alternative model organisms for toxicological fingerprinting of relevant parameters in food and nutrition. *Crit. Rev. Food Sci. Nutr.* **2022**, *62*, 5965–5982. [CrossRef] [PubMed]
84. Wang, J.; Liu, H.; Shi, X.; Qin, S.; Liu, J.; Lv, Q.; Liu, J.; Li, Q.; Wang, Z.; Wang, L. Development and application of an advanced biomedical material—Silk sericin. *Adv. Mater.* **2024**, *36*, 2311593. [CrossRef] [PubMed]
85. Arango, M.C.; Montoya, Y.; Peresin, M.S.; Bustamante, J.; Álvarez-López, C. Silk sericin as a biomaterial for tissue engineering: A review. *Int. J. Polym. Mater. Polym. Biomater.* **2021**, *70*, 1115–1129. [CrossRef]

86. Lüdtke, F.L.; Silva, T.J.; da Silva, M.G.; Hashimoto, J.C.; Ribeiro, A.P.B. Lipid nanoparticles: Formulation, production methods and characterization protocols. *Foods* **2025**, *14*, 973. [CrossRef] [PubMed]
87. McClements, D.J.; Rao, J. Food-grade nanoemulsions: Formulation, fabrication, properties, performance, biological fate, and potential toxicity. *Crit. Rev. Food Sci. Nutr.* **2011**, *51*, 285–330. [CrossRef] [PubMed]
88. Izza, N.; Watanabe, N.; Okamoto, Y.; Suga, K.; Wibisono, Y.; Kajimura, N.; Mitsuoka, K.; Umakoshi, H. Dependence of the core–shell structure on the lipid composition of nanostructured lipid carriers: Implications for drug carrier design. *ACS Appl. Nano Mater.* **2022**, *5*, 9958–9969. [CrossRef]
89. Alloush, T.; Demiralp, B. A review of formulation strategies for cyclodextrin-enhanced solid lipid nanoparticles (SLNs) and nanostructured lipid carriers (NLCs). *Int. J. Mol. Sci.* **2025**, *26*, 6509. [CrossRef] [PubMed]
90. Pochapski, D.J.; Carvalho dos Santos, C.; Leite, G.W.; Pulcinelli, S.H.; Santilli, C.V. Zeta potential and colloidal stability predictions for inorganic nanoparticle dispersions: Effects of experimental conditions and electrokinetic models on the interpretation of results. *Langmuir* **2021**, *37*, 13379–13389. [CrossRef] [PubMed]
91. Punia, S.; Kumar, M.; Sandhu, K.S.; Whiteside, W.S. Rice-bran oil: An emerging source of functional oil. *J. Food Process. Preserv.* **2021**, *45*, e15318. [CrossRef]
92. Saez, V.; Souza, I.D.L.; Mansur, C.R.E. Lipid nanoparticles (SLN & NLC) for delivery of vitamin E: A comprehensive review. *Int. J. Cosmet. Sci.* **2018**, *40*, 103–116. [CrossRef] [PubMed]
93. Tang, C.H.; Chen, H.L.; Dong, J.R. Solid lipid nanoparticles (SLNs) and nanostructured lipid carriers (NLCs) as food-grade nanovehicles for hydrophobic nutraceuticals or bioactives. *Appl. Sci.* **2023**, *13*, 1726. [CrossRef]
94. Honary, S.; Zahir, F. Effect of zeta potential on the properties of nano-drug delivery systems—A review (Part 2). *Trop. J. Pharm. Res.* **2013**, *12*, 265–273. [CrossRef]
95. Schmid-Wendtner, M.H.; Korting, H.C. The pH of the skin surface and its impact on the barrier function. *Ski. Pharmacol. Physiol.* **2006**, *19*, 296–302. [CrossRef] [PubMed]
96. Weiser, J.R.; Saltzman, W.M. Controlled release for local delivery of drugs: Barriers and models. *J. Control. Release* **2014**, *190*, 664–673. [CrossRef] [PubMed]
97. Wu, K.W.; Sweeney, C.; Dudhipala, N.; Lakhani, P.; Chaurasiya, N.D.; Tekwani, B.L.; Majumdar, S. Primaquine loaded solid lipid nanoparticles (SLN), nanostructured lipid carriers (NLC), and nanoemulsion (NE): Effect of lipid matrix and surfactant on drug entrapment, in vitro release, and ex vivo hemolysis. *AAPS PharmSciTech* **2021**, *22*, 240. Correction in *AAPS PharmSciTech* **2021**, *23*, 30. https://doi.org/10.1208/s12249-021-02171-y. [CrossRef] [PubMed]
98. Amnuaykan, P.; Anantaworasakul, P.; Lueadnakrob, K.; Kunkul, P.; Chokrungsarid, W.; Thummanuwong, A.; Juntrapirom, S.; Kanjanakawinkul, W.; Chaiyana, W. Nanostructured lipid carriers for sustained release and enhanced delivery of *Vanda coerulea* protocorm extract. *Pharmaceutics* **2025**, *17*, 1076. [CrossRef] [PubMed]
99. Kichou, H.; Bonnier, F.; Dancik, Y.; Bakar, J.; Michael-Jubeli, R.; Caritá, A.C.; Perse, X.; Soucé, M.; Rapetti, L.; Tfayli, A.; et al. Strat-M® positioning for skin permeation studies: A comparative study including EpiSkin® RHE and human skin. *Int. J. Pharm.* **2023**, *647*, 123488. [CrossRef] [PubMed]
100. Zoio, P.; Lopes-Ventura, S.; Marto, J.; Oliva, A. Open-source human skin model with an in vivo-like barrier for drug testing. *ALTEX* **2022**, *39*, 405–418. [CrossRef] [PubMed]
101. Haq, A.; Goodyear, B.; Ameen, D.; Joshi, V.; Michniak-Kohn, B. Strat-M® synthetic membrane: Permeability comparison to human cadaver skin. *Int. J. Pharm.* **2018**, *547*, 432–437. [CrossRef] [PubMed]
102. Carlos da Silva, G.; Barbosa, M.B.; Júnior, F.B.C.; Moreira, P.L.; Werka, R.; Martin, A.A. Detection of skin wrinkles and quantification of roughness using a novel image processing technique from a dermatoscope device. *Ski. Res. Technol.* **2023**, *29*, e13335. [CrossRef] [PubMed]
103. Gougeon, S.; Hernandez, E.; Chevrot, N.; Vergne, T.; Cherel, M.; Prestat-Marquis, E.; Jomier, M.; Burty-Valin, E. Evaluation of a new connected portable camera for the analysis of skin microrelief and the assessment of the effect of skin moisturisers. *Ski. Res. Technol.* **2023**, *29*, e13190. [CrossRef] [PubMed]

Disclaimer/Publisher's Note: The statements, opinions and data contained in all publications are solely those of the individual author(s) and contributor(s) and not of MDPI and/or the editor(s). MDPI and/or the editor(s) disclaim responsibility for any injury to people or property resulting from any ideas, methods, instructions or products referred to in the content.